Supplement of Geosci. Model Dev., 18, 6805–6834, 2025
https://doi.org/10.5194/gmd-18-6805-2025-supplement

Geoscientific Model Development
Open Access
EGU

Supplement of

NutGEnIE 1.0: nutrient cycle extensions to the cGEnIE Earth system model to examine the long-term influence of nutrients on oceanic primary production

David A. Stappard et al.

Correspondence to: David A. Stappard (ds2n19@soton.ac.uk)

S1. Supplementary analysis

S1.1. Apparent Oxygen Utilisation (AOU) analysis

Apparent Oxygen Utilization (AOU) is the difference between the amount of oxygen that would be dissolved in seawater at a given temperature and salinity if it were in equilibrium with the atmosphere and the actual measured amount of dissolved oxygen. It can indicate how much oxygen has been consumed by biological activity, primarily through respiration/remineralisation, as water has circulated through the deep ocean since it lest the surface. The WOA 2018 provides an AOU annual climatology dataset (Garcia et al., 2018) which was re-gridded to match the NutGEnIE grid dimensions. For NutGEnIE oxygen saturation values were calculated based on temperature and salinity following the method and parameters of Garcia and Gordon (1992) to facilitated calculation of ocean AOU values.

Thermohaline transects of AOU for WOAG and NutGEnIE are provided in Fig. S50 and S51 respectively. The overall pattern and magnitude of AOU is well aligned between WOAG and NutGEnIE with values increasing along the thermohaline transect and reaching maximum values in the North Pacific. There are some noteworthy differences NutGEnIE AOU values in the Arctic are higher, particularly at depth below 2 000 m, in addition, NutGEnIE AOU values in the North Pacific are lower particular at depth between 200 and 1 000 m.

S1.2. Nitrogen* (N^*) analysis

Nitrogen* (N^*) is a tracer to examine the impact of nitrogen fixation and denitrification on oceanic NO_3 distributions. This is achieved by removing the 16:1 trend of photosynthesis/remineralisation, allowing focus to be given to anomalies from this trend. A linear combination of the two nutrients nitrate and phosphate, N^*, is then defined as Eq. (S1) where the constant of 2.9 μmol kg^{-1} is set to obtain a global mean N^* of zero (Gruber and Sarmiento, 1997). It should be noted that N^* does not give a measure of either nitrogen fixation or denitrification but the sum of these two processes.

$$N^* = [NO_3] - 16[PO_4] + 2.9\ \mu mol\ kg^{-1} \quad \text{(S1)}$$

N^* values are calculated for both the WOAG and NutGEnIE based on NO_3 and PO_4 concentrations and provided in Fig. S52 and S53 respectively. The overall trend in N^* for both WOAG and NutGEnIE is that concentrations are highest in the North Atlantic and decrease gradually toward the Pacific. For both WOAG and NutGEnIE this implies a net transport of fixed nitrogen from the Atlantic to the Pacific. There are aspects of WOAG N^* that are not represented by NutGEnIE, for example NutGEnIE has universally negative values of N^* along the pacific transect whereas WOAG has some positive values in the upper water column.

S1.3. Model tuning

It has been stated in the main manuscript that a significant tuning exercise was undertaken. Details of this process are provided within the model data repository in folder 07 Tuning, see the Data availability section of the main manuscript for location of

the repository. An excel spreadsheet is provided where the first tab details the parameters values that were set for each run of the turning exercise, the second tab details summary outputs including tracer concentrations and process rates.

S2. Supplementary figures

S2.1. Nutrient flux distributions

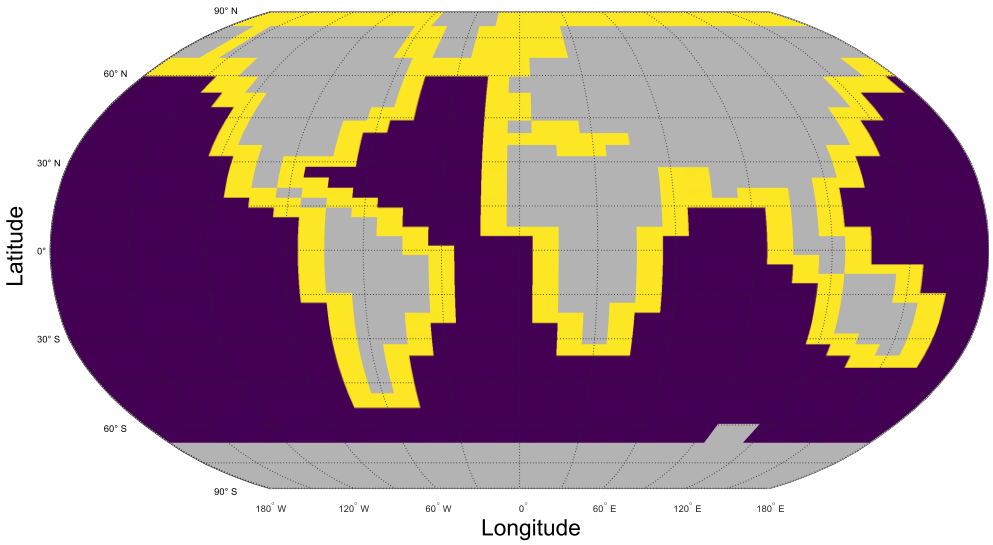

Figure S1 Spatial distribution of surface nutrient input fluxes. This spatial distribution is applied to riverine phosphate (RP) and riverine nitrate (RN). Those cells adjacent to land (excluding Antarctica) and coloured yellow receive the input flux; all other cells, coloured dark blue, do not receive the input flux. The total input flux is distributed evenly to those cells (coloured yellow) that receive it.

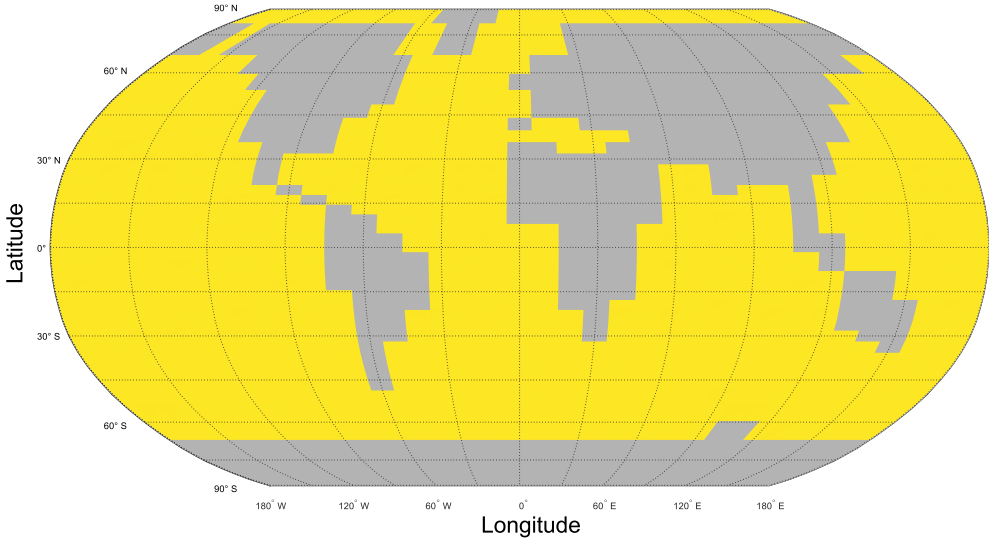

Figure S2 Spatial distribution of seafloor nutrient input flux. This spatial distribution is applied to benthic (seafloor) iron (BFe). All cells immediately above the seafloor receive the input flux. The total input flux is distributed evenly to those cells (coloured yellow) that receive it.

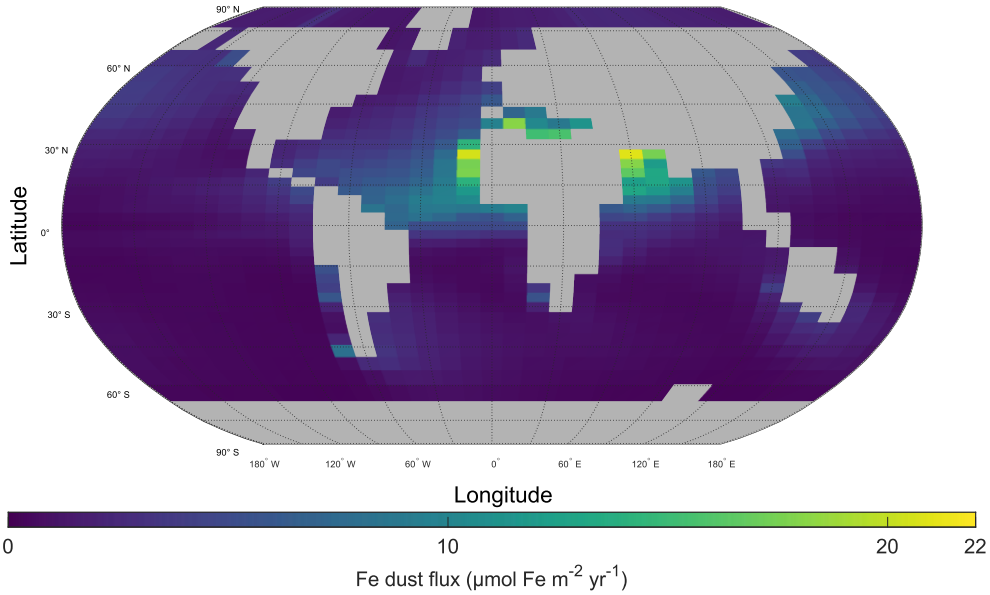

Figure S3 Spatial distribution of surface dust input flux of iron. This spatial distribution is applied to dust iron (DDFe). All cells at the surface receive the input flux, but in greatly varying degrees according to the colour shown (distribution based on a re-gridding from Mahowald et al. (2006)). The implementation in NutGEnIE is as described in Matsumoto et al. (2013) The total input flux is distributed unevenly across the ocean surface, with little or none going to those cells coloured dark blue and large amounts to those coloured yellow.

S2.2. Age of water.

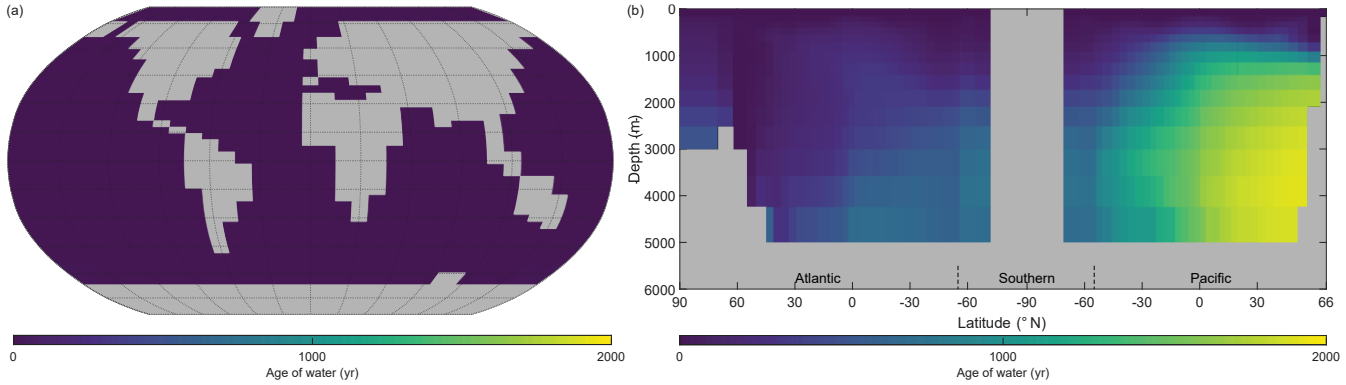

Figure S4 Annual mean age of water (years since ventilation). (a) NutGEnIE surface, as surface layer is in contact with atmosphere age is zero for all cells. (b) NutGEnIE thermohaline transect zonal mean.

S2.3. Spin up experiment end state.

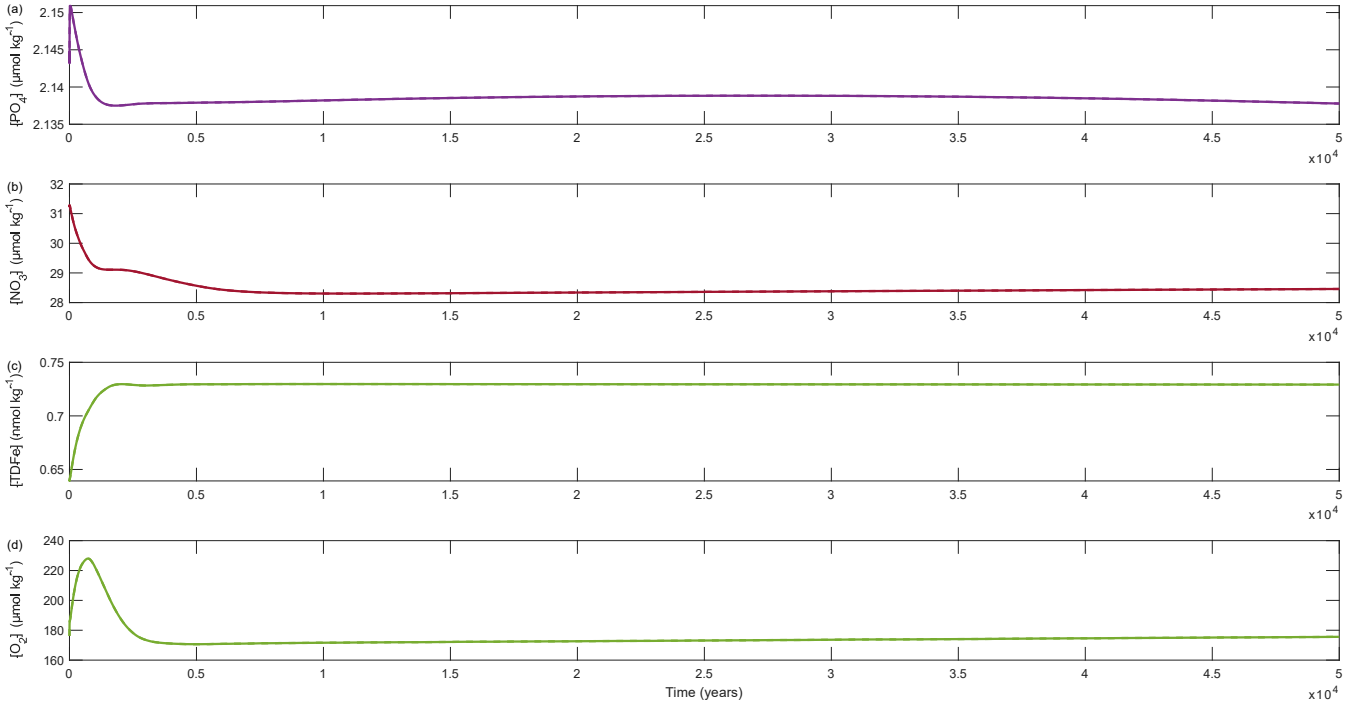

Figure S5 Concentrations of nutrients and dissolved oxygen during 50 kyr NutGEnIE spin up experiment. (a) global mean [PO_4] μmol kg^{-1}. (b) global mean [NO_3] μmol kg^{-1}. (c) global mean [TDFe] nmol kg^{-1}. (d) global mean [O_2] μmol kg^{-1}.

S2.4. Iron depth profiles.

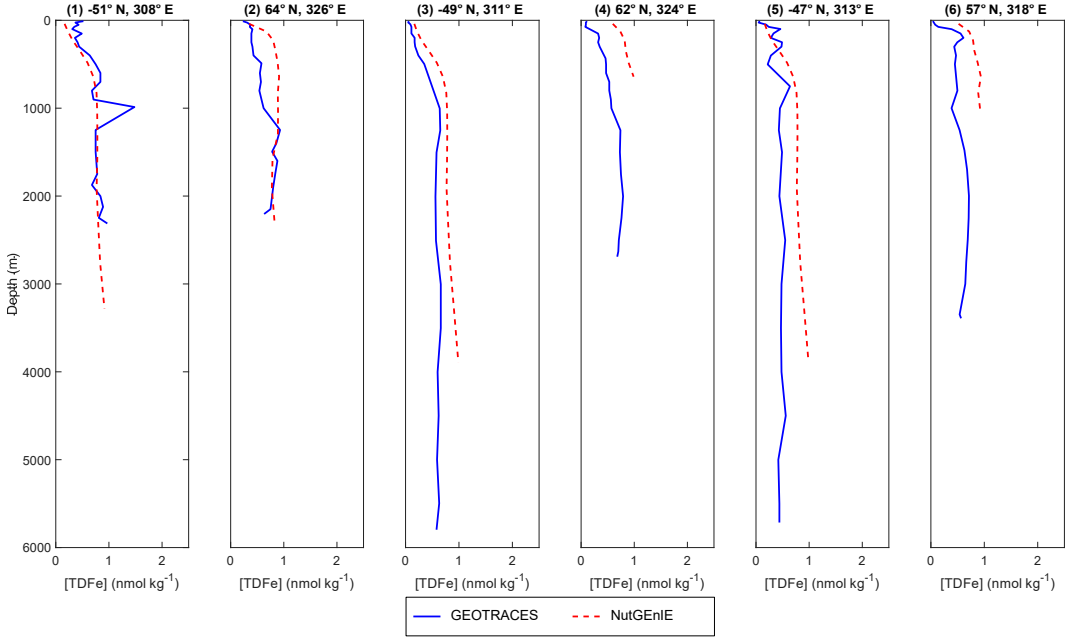

Figure S6 Iron depth profiles for GEOTRACES cruise GA02 1 of 8. Total dissolved iron (TDFe) in nmol kg^{-1}. Blue line represents GEOTRACES observations of [TDFe], red dashed line represents NutGEnIE [TDFe].

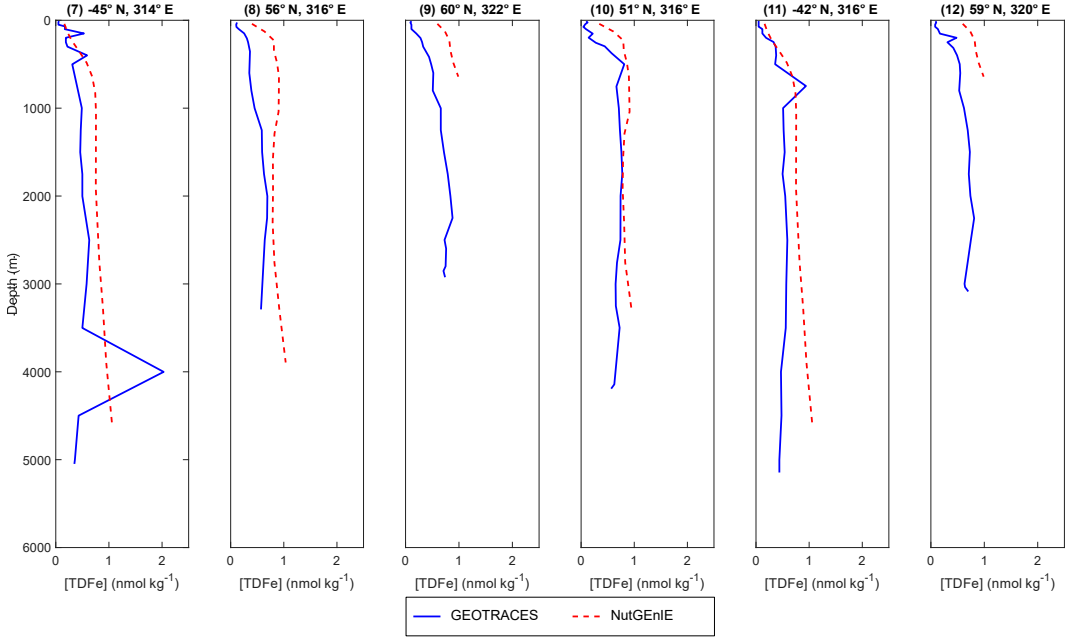

Figure S7 Iron depth profiles for GEOTRACES cruise GA02 2 of 8. Total dissolved iron (TDFe) in nmol kg^{-1}. Blue line represents GEOTRACES observations of [TDFe], red dashed line represents NutGEnIE [TDFe].

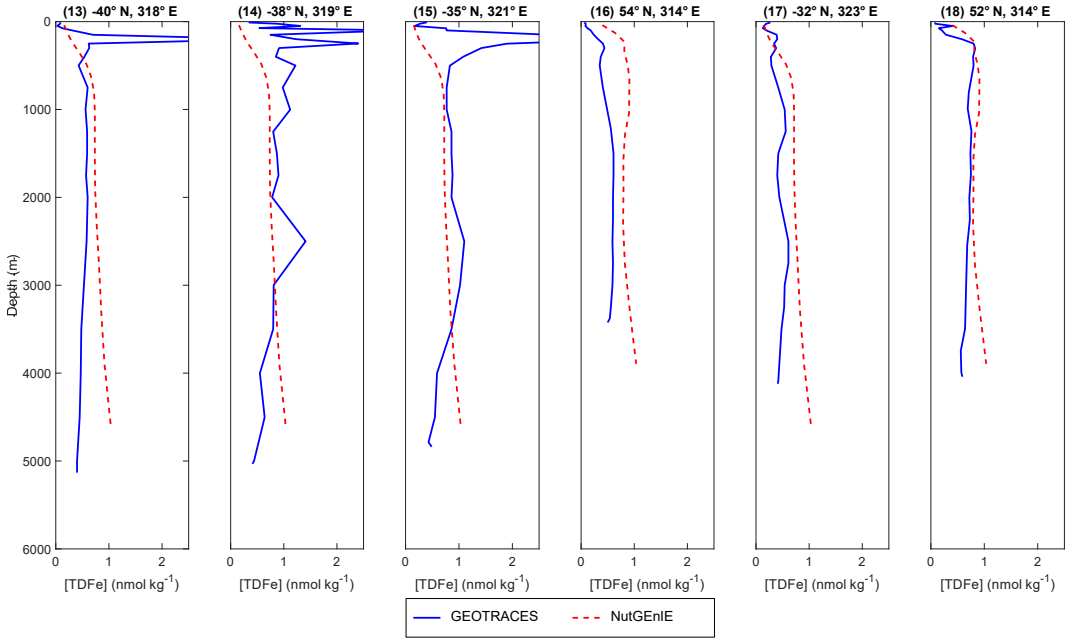

Figure S8 Iron depth profiles for GEOTRACES cruise GA02 3 of 8. Total dissolved iron (TDFe) in nmol kg^{-1}. Blue line represents GEOTRACES observations of [TDFe], red dashed line represents NutGEnIE [TDFe].

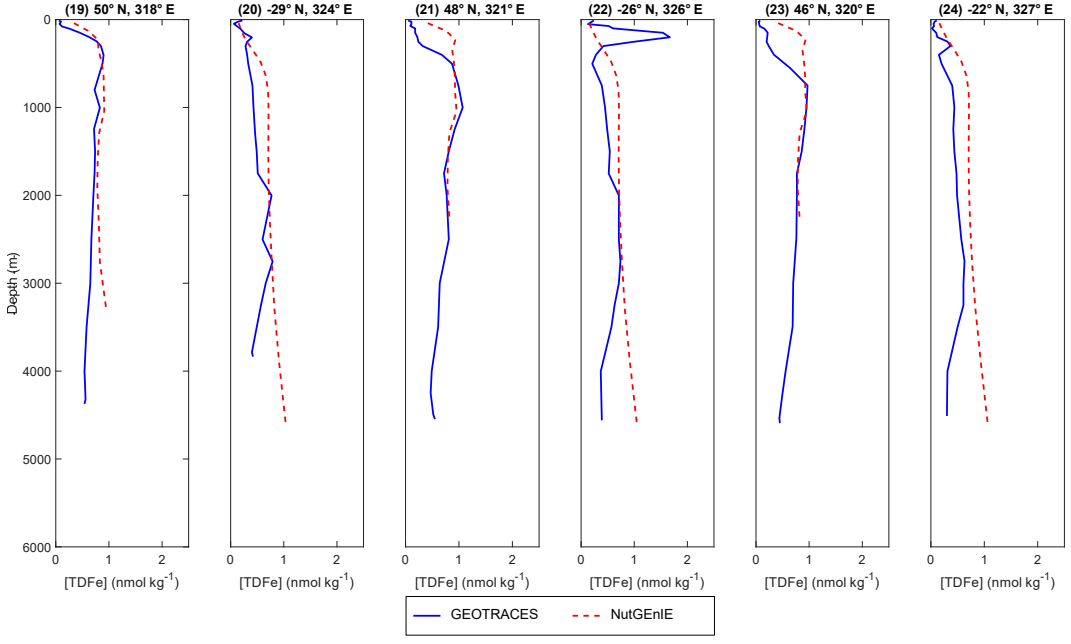

Figure S9 Iron depth profiles for GEOTRACES cruise GA02 4 of 8. Total dissolved iron (TDFe) in nmol kg^{-1}. Blue line represents GEOTRACES observations of [TDFe], red dashed line represents NutGEnI [TDFe].

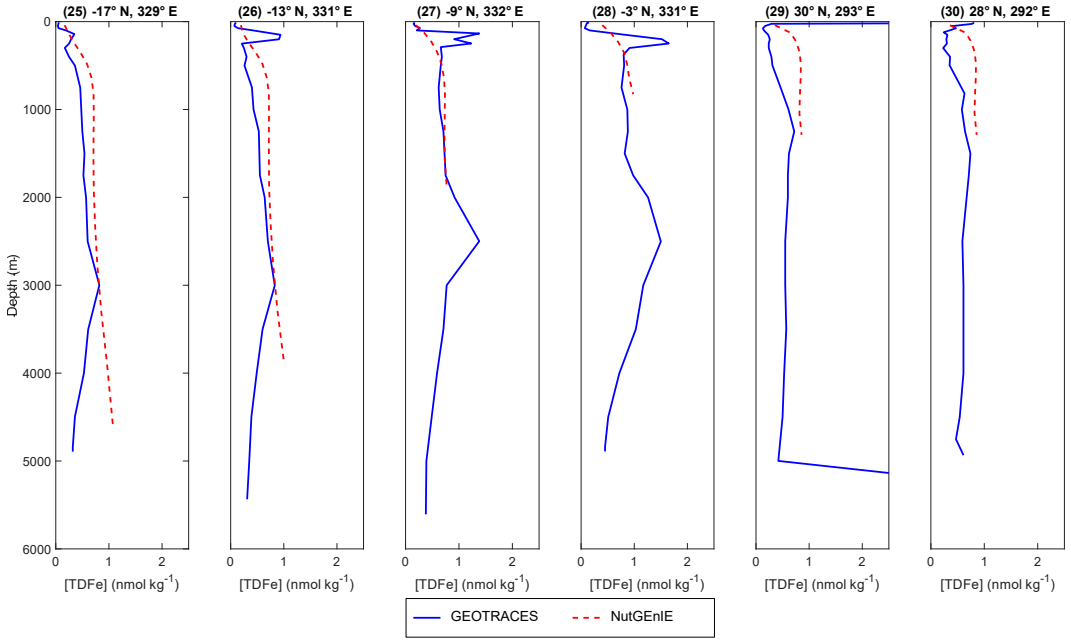

Figure S10 Iron depth profiles for GEOTRACES cruise GA02 5 of 8. Total dissolved iron (TDFe) in nmol kg^{-1}. Blue line represents GEOTRACES observations of [TDFe], red dashed line represents NutGEnIE [TDFe].

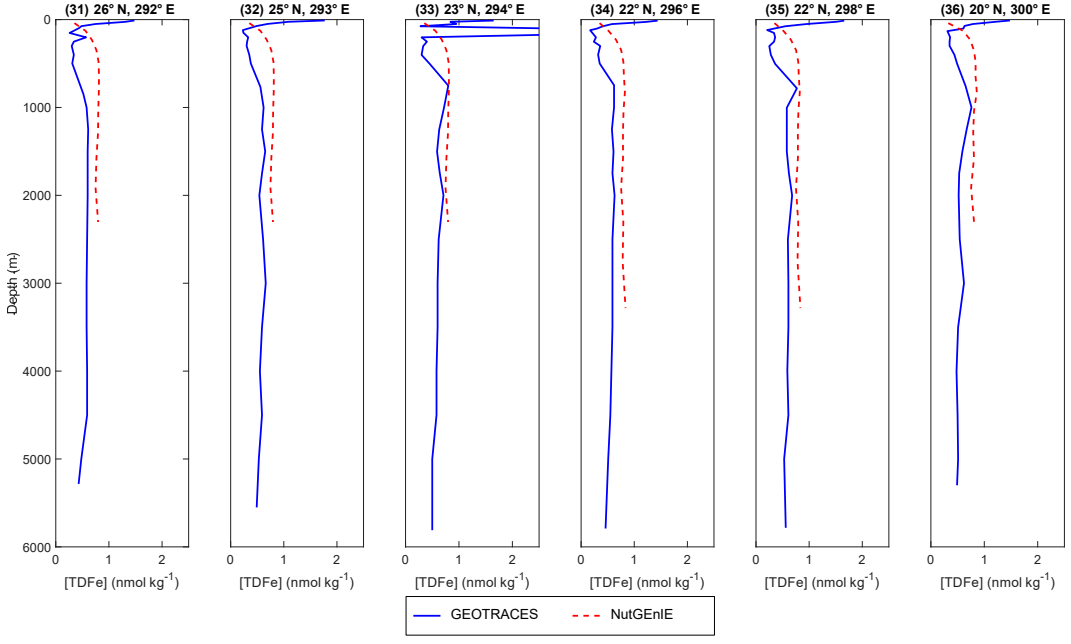

Figure S11 Iron depth profiles for GEOTRACES cruise GA02 6 of 8. Total dissolved iron (TDFe) in nmol kg^{-1}. Blue line represents GEOTRACES observations of [TDFe], red dashed line represents NutGEnIE [TDFe].

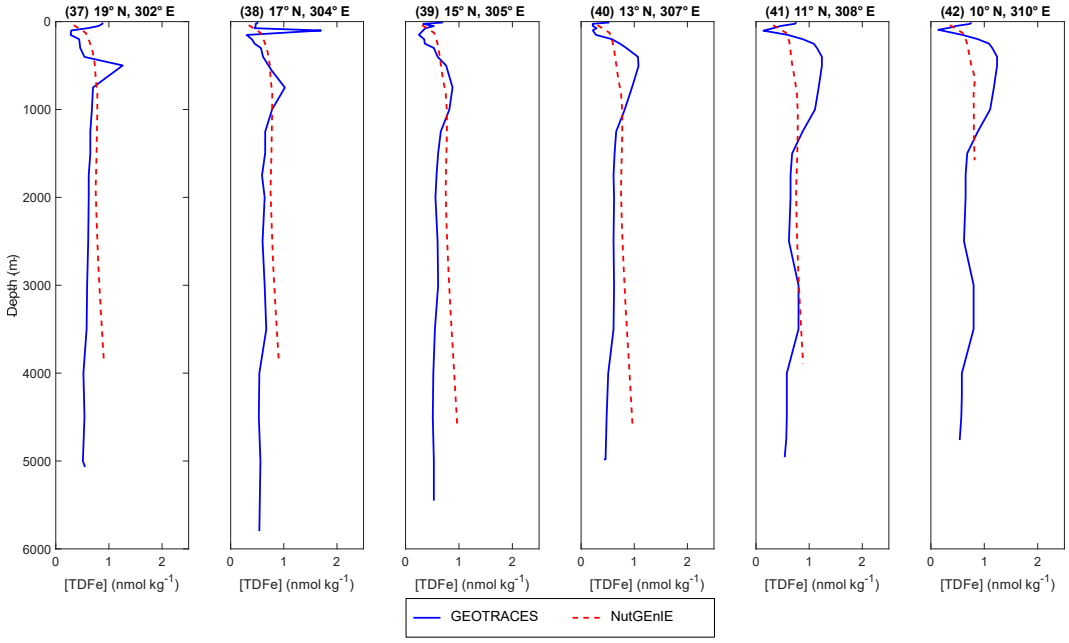

Figure S12 Iron depth profiles for GEOTRACES cruise GA02 7 of 8. Total dissolved iron (TDFe) in nmol kg^{-1}. Blue line represents GEOTRACES observations of [TDFe], red dashed line represents NutGEnIE [TDFe].

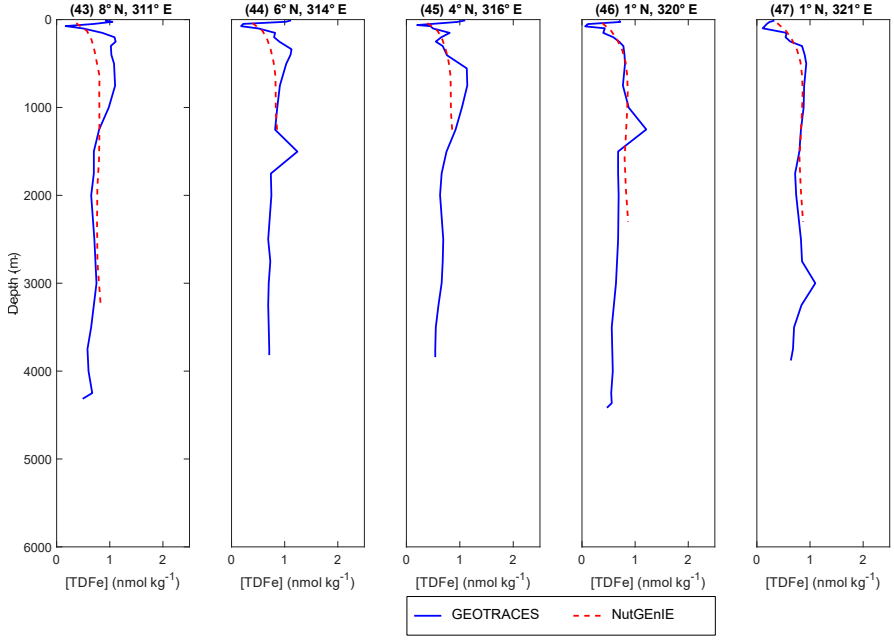

80

Figure S13 Iron depth profiles for GEOTRACES cruise GA02 8 of 8. Total dissolved iron (TDFe) in nmol kg^{-1}. Blue line represents GEOTRACES observations of [TDFe], red dashed line represents NutGEnIE [TDFe].

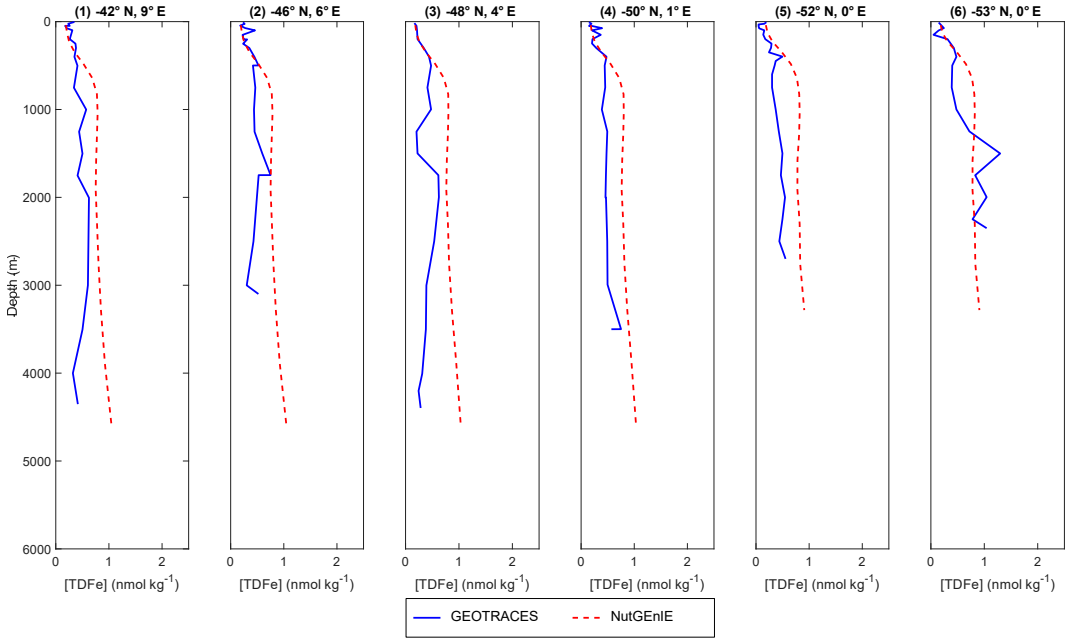

Figure S14 Iron depth profiles for GEOTRACES cruise GIPY05 1 of 6. Total dissolved iron (TDFe) in nmol kg^{-1}. Blue line represents GEOTRACES observations of [TDFe], red dashed line represents NutGEnIE [TDFe].

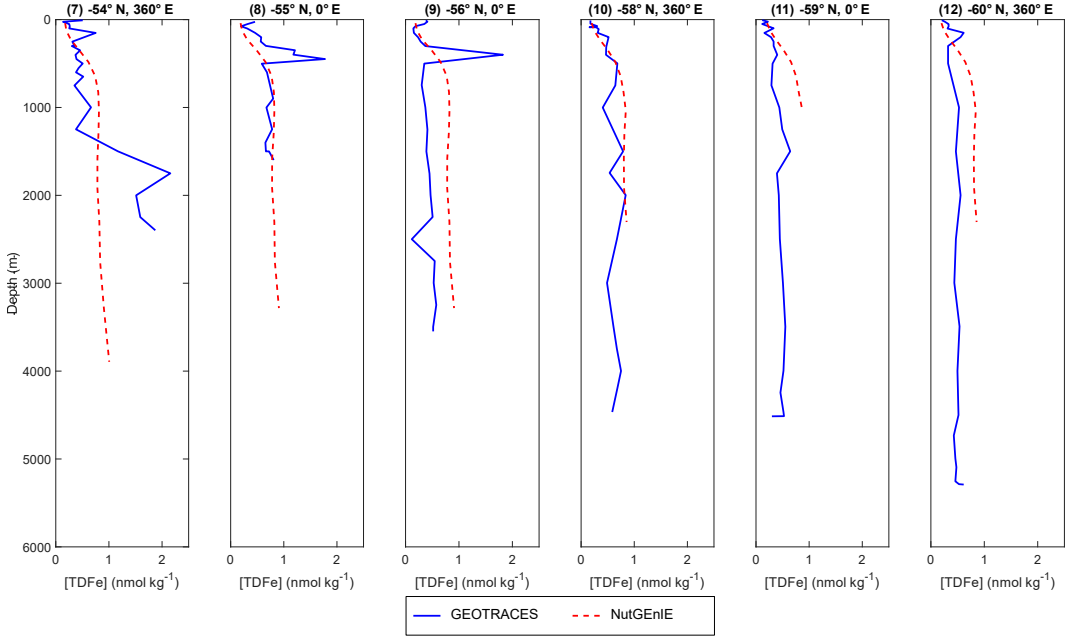

Figure S15 Iron depth profiles for GEOTRACES cruise GIPY05 2 of 6. Total dissolved iron (TDFe) in nmol kg^{-1}. Blue line represents GEOTRACES observations of [TDFe], red dashed line represents NutGEnIE [TDFe].

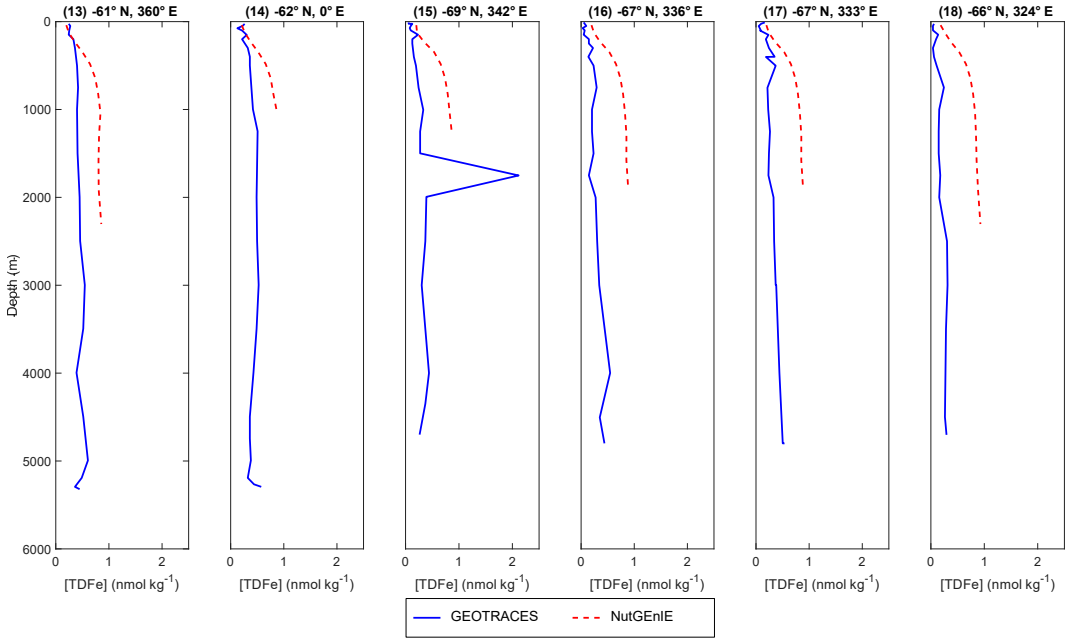

Figure S16 Iron depth profiles for GEOTRACES cruise GIPY05 3 of 6. Total dissolved iron (TDFe) in nmol kg^{-1}. Blue line represents GEOTRACES observations of [TDFe], red dashed line represents NutGEnIE [TDFe].

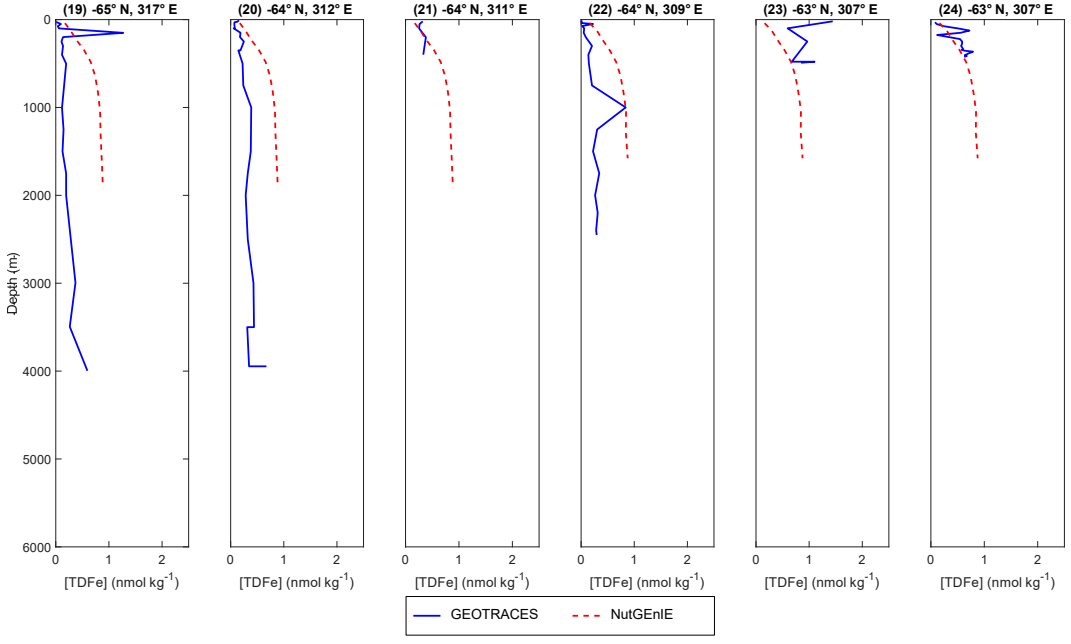

Figure S17 Iron depth profiles for GEOTRACES cruise GIPY05 4 of 6. Total dissolved iron (TDFe) in nmol kg^{-1}. Blue line represents GEOTRACES observations of [TDFe], red dashed line represents NutGEnIE [TDFe].

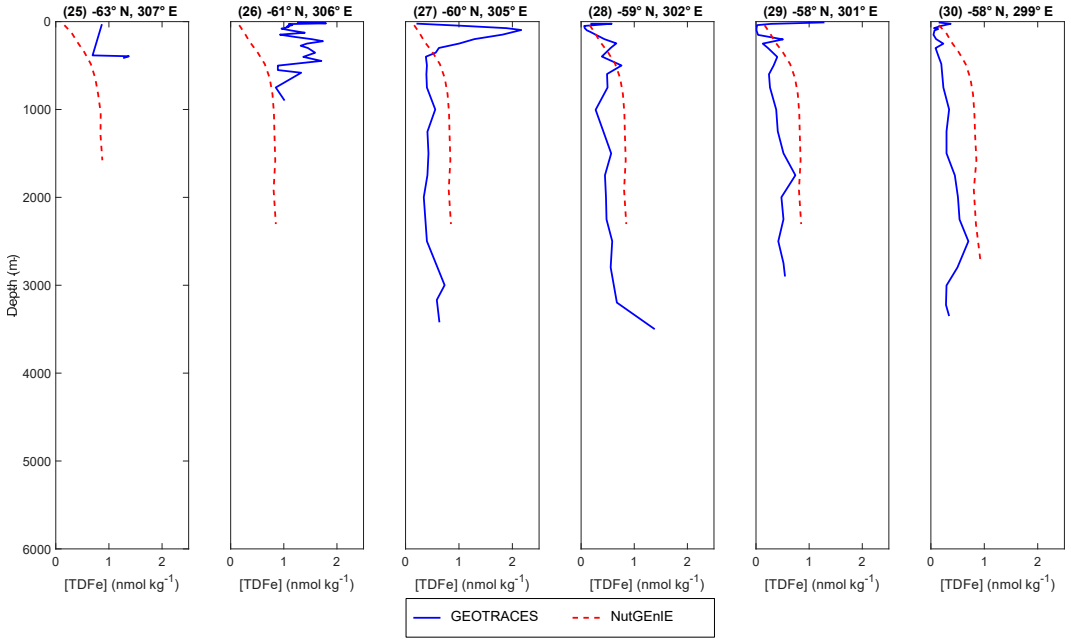

Figure S18 Iron depth profiles for GEOTRACES cruise GIPY05 5 of 6. Total dissolved iron (TDFe) in nmol kg^{-1}. Blue line represents GEOTRACES observations of [TDFe], red dashed line represents NutGEnIE [TDFe].

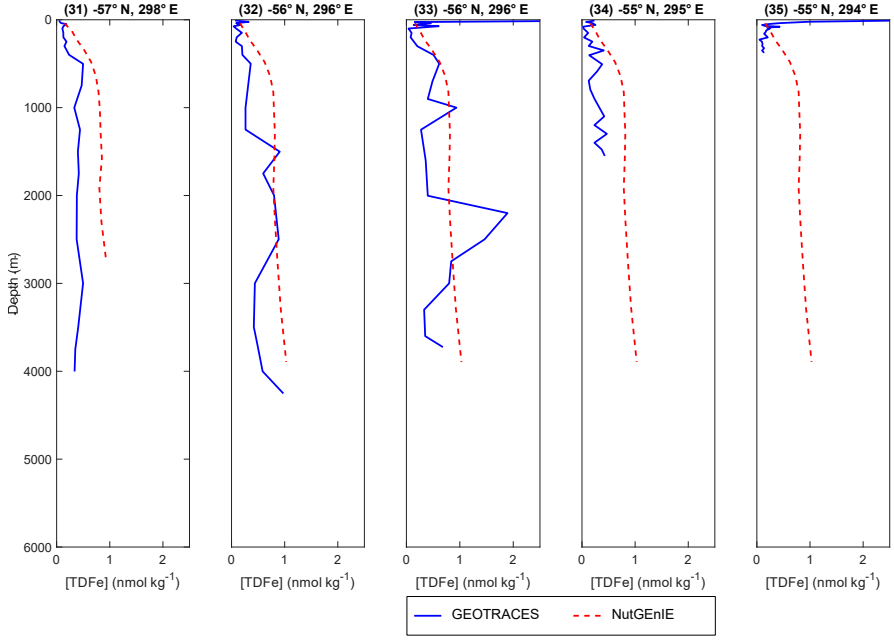

Figure S19 Iron depth profiles for GEOTRACES cruise GIPY05 6 of 6. Total dissolved iron (TDFe) in nmol kg^{-1}. Blue line represents GEOTRACES observations of [TDFe], red dashed line represents NutGEnIE [TDFe].

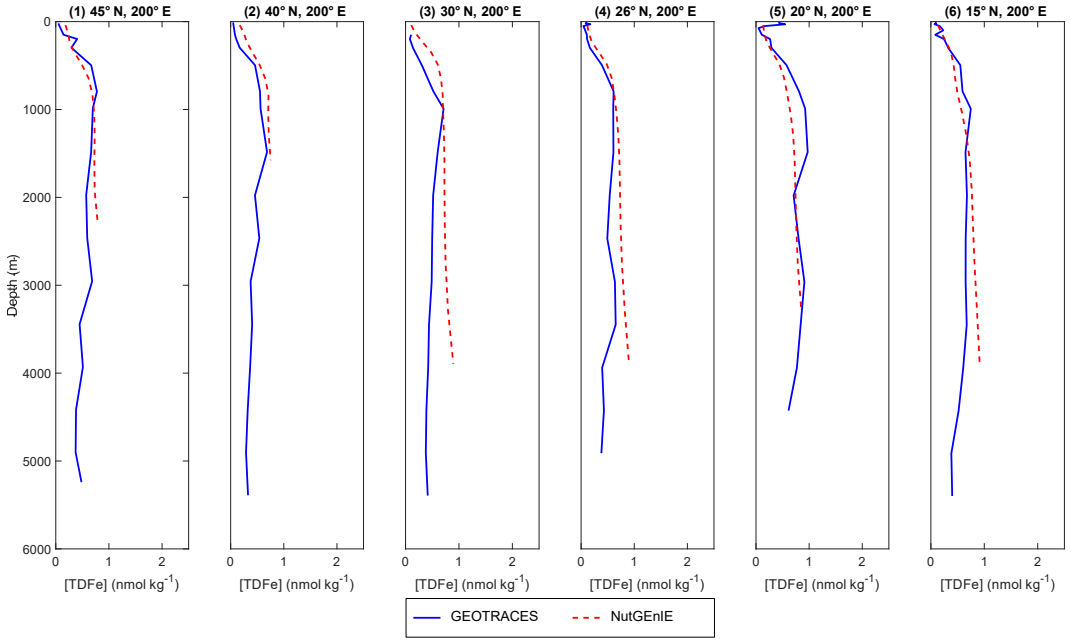

Figure S20 Iron depth profiles for GEOTRACES cruise GPc06 1 of 2. Total dissolved iron (TDFe) in nmol kg^{-1}. Blue line represents GEOTRACES observations of [TDFe], red dashed line represents NutGEnIE [TDFe].

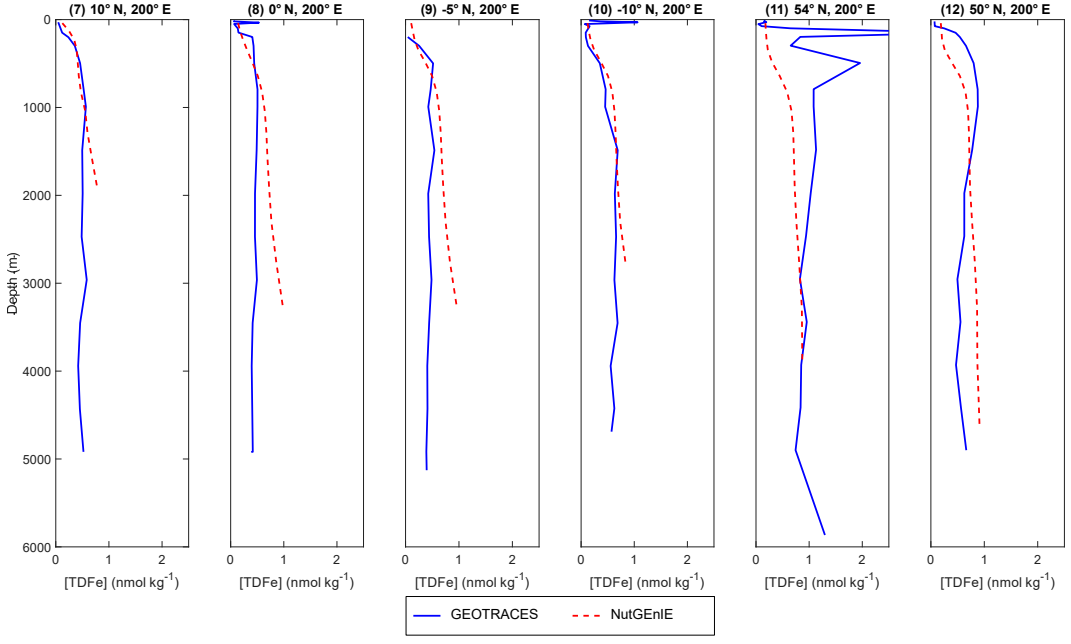

Figure S21 Iron depth profiles for GEOTRACES cruise GPc06 2 of 2. Total dissolved iron (TDFe) in nmol kg^{-1}. Blue line represents GEOTRACES observations of [TDFe], red dashed line represents NutGEnIE [TDFe].

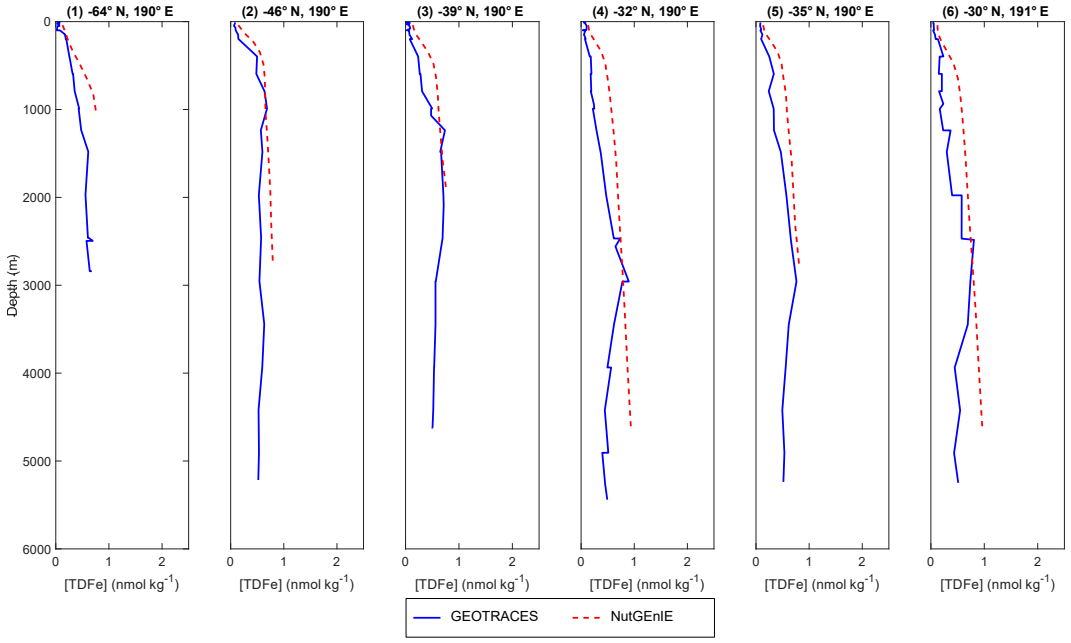

Figure S22 Iron depth profiles for GEOTRACES cruise GP19 1 of 3. Total dissolved iron (TDFe) in nmol kg^{-1}. Blue line represents GEOTRACES observations of [TDFe], red dashed line represents NutGEnIE [TDFe].

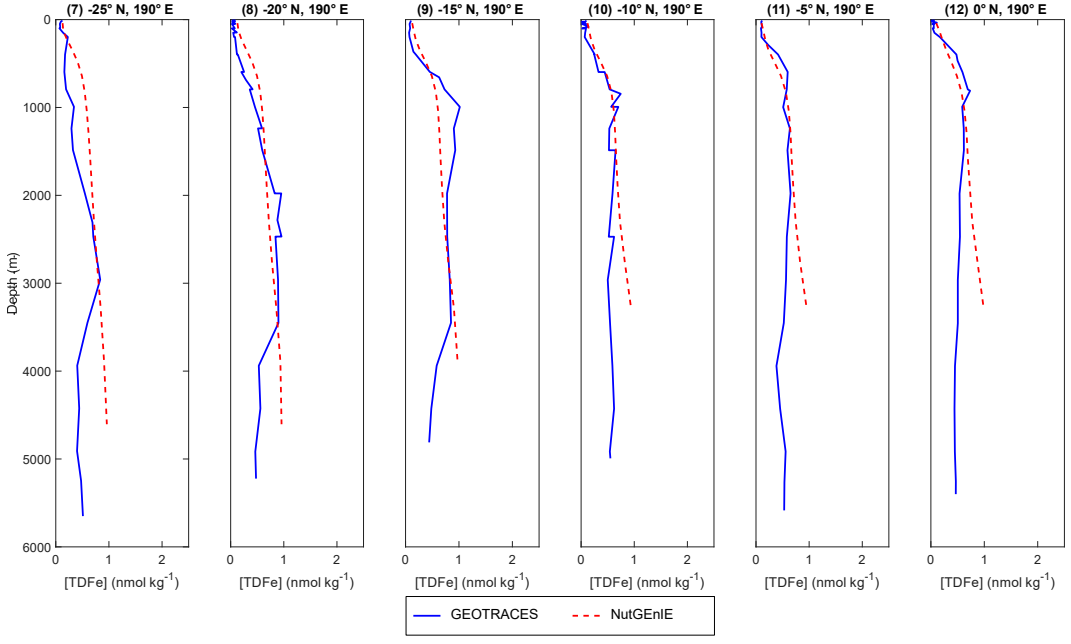

Figure S23 Iron depth profiles for GEOTRACES cruise GP19 2 of 3. Total dissolved iron (TDFe) in nmol kg^{-1}. Blue line represents GEOTRACES observations of [TDFe], red dashed line represents NutGEnIE [TDFe].

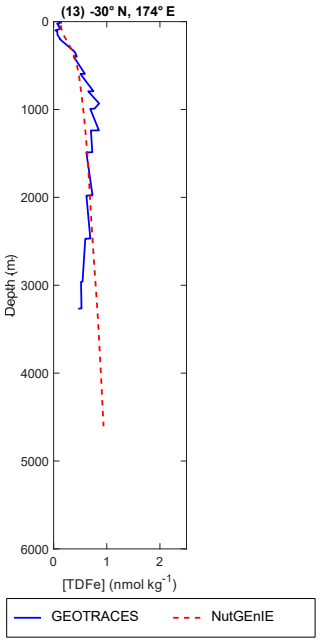

Figure S24 Iron depth profiles for GEOTRACES cruise GP19 3 of 3. Total dissolved iron (TDFe) in nmol kg^{-1}. Blue line represents GEOTRACES observations of [TDFe], red dashed line represents NutGEnIE [TDFe].

S2.5. NutGEnIE iron spatial distributions

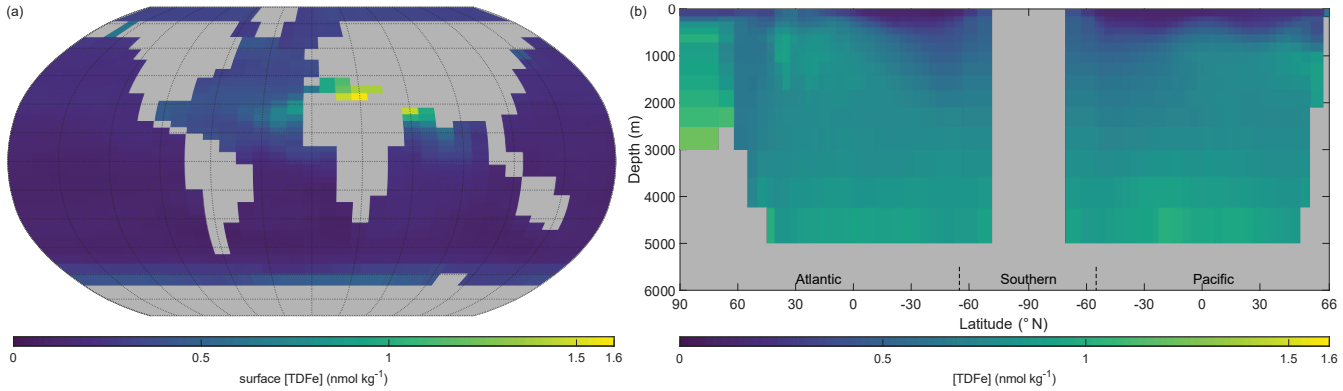

Figure S25 Annual mean global iron concentration ([TDFe]). (a) NutGEnIE surface [TDFe]. (b) NutGEnIE thermohaline transect zonal mean [TDFe]. [TDFe] in nmol kg^{-1}.

S2.6. Statistical validation – histograms.

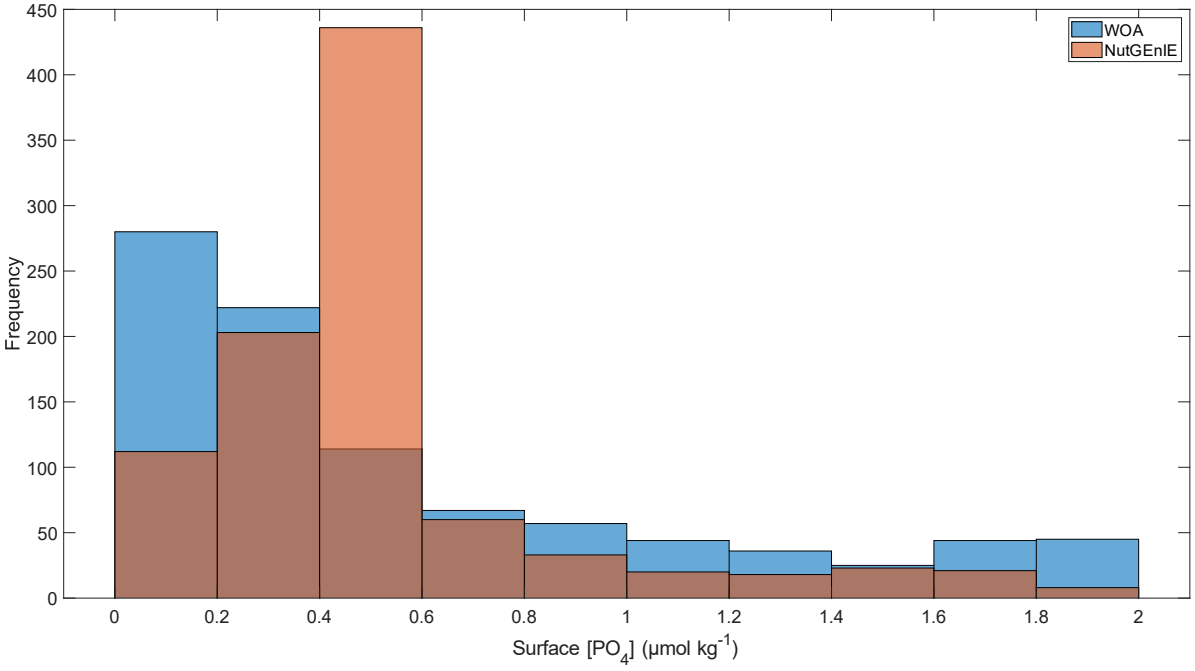

Figure S26 Histogram of NutGEnIE and WOA surface [PO_4^{3-}]. NutGEnIE shown in orange, WOA shown in blue. Concentration values in µmol kg^{-1}.

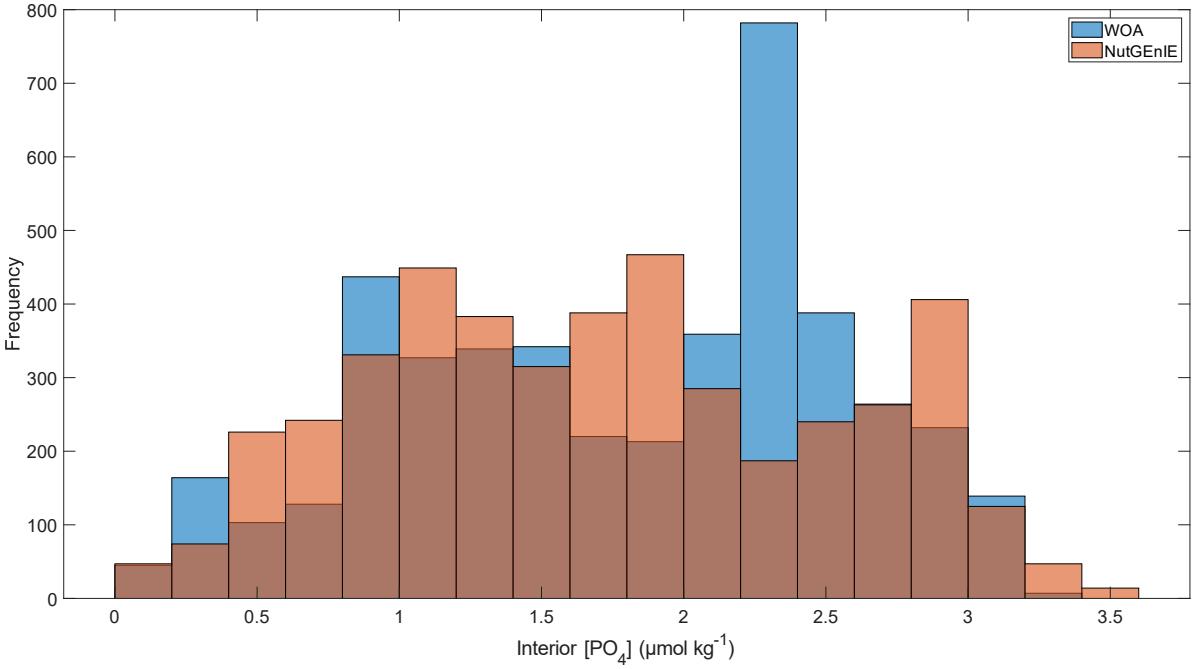

Figure S27 Histogram of NutGEnIE and WOA interior [PO_4^{3-}]. NutGEnIE shown in orange, WOA shown in blue. Concentration values in µmol kg^{-1}.

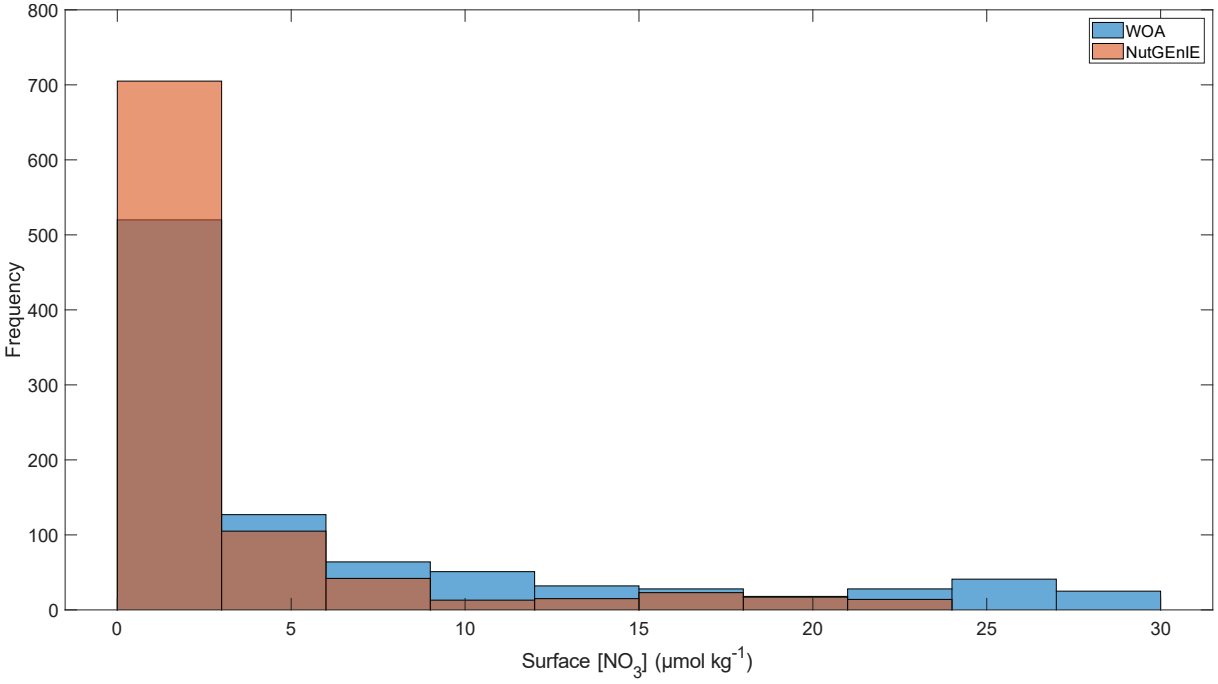

Figure S28 Histogram of NutGEnIE and WOA surface [NO_3^-]. NutGEnIE shown in orange, WOA shown in blue. Concentration values in µmol kg^{-1}.

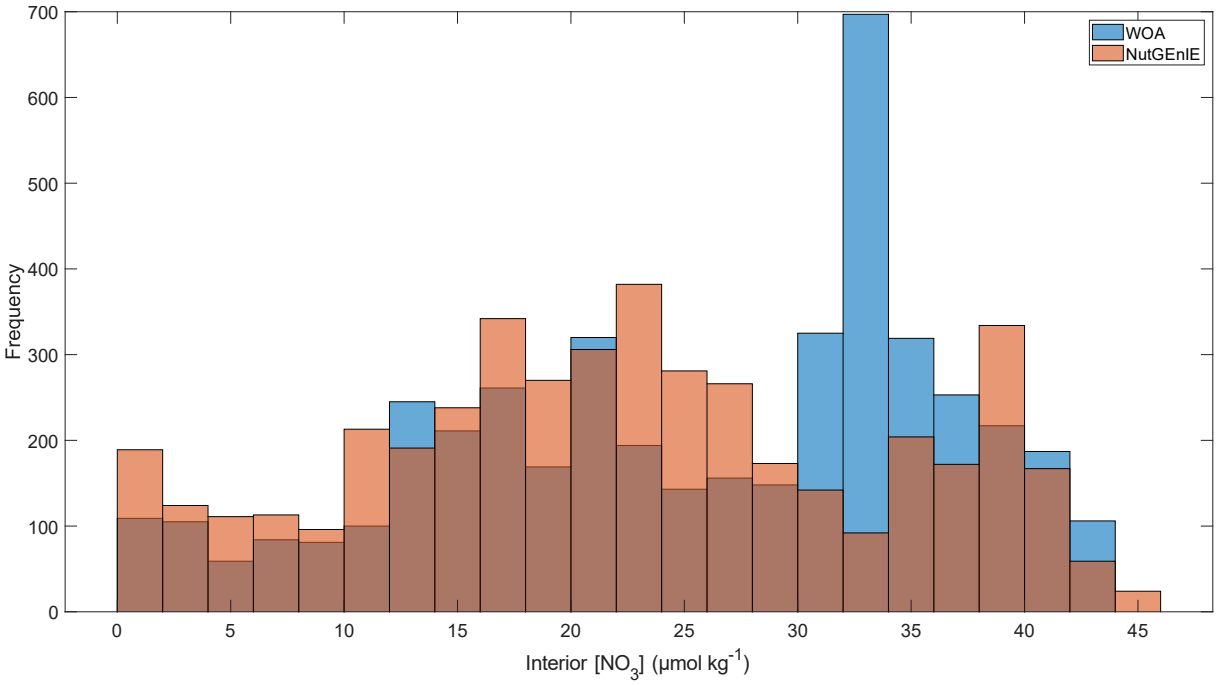

Figure S29 Histogram of NutGEnIE and WOA interior [NO_3^-]. NutGEnIE shown in orange, WOA shown in blue. Concentration values in µmol kg^{-1}.

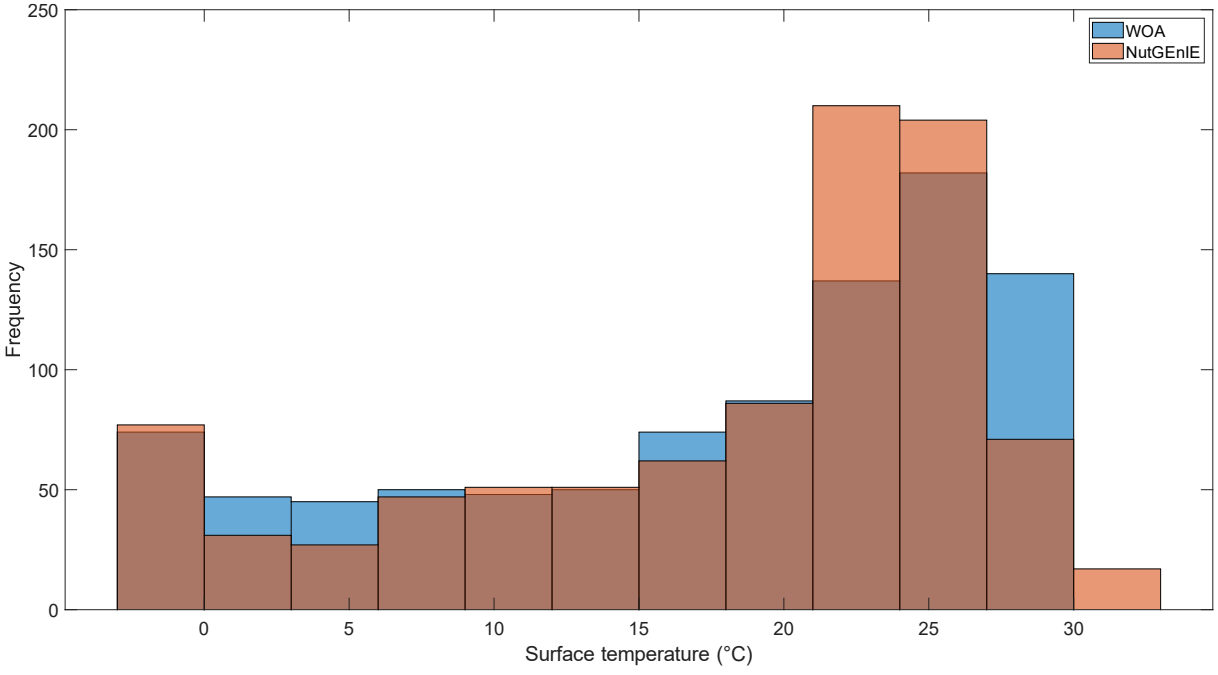

135 **Figure S30 Histogram of NutGEnIE and WOA surface temperature.** NutGEnIE shown in orange, WOA shown in blue. Temperature values in °C.

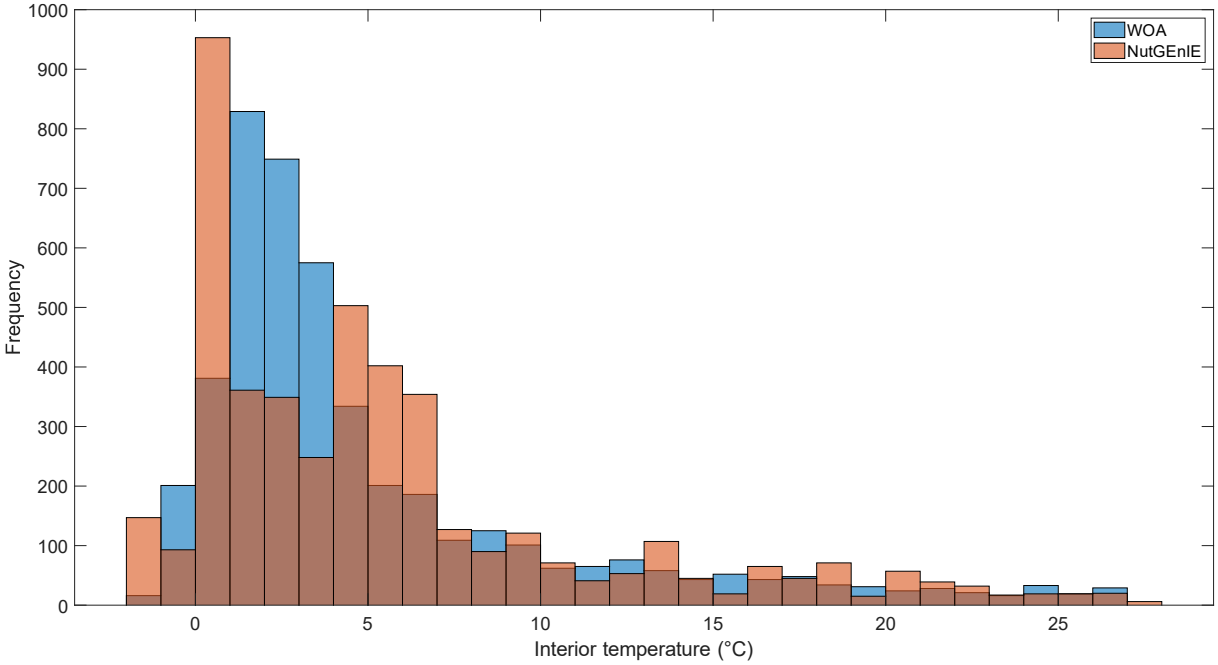

Figure S31 Histogram of NutGEnIE and WOA interior temperature. NutGEnIE shown in orange, WOA shown in blue. Temperature values in °C.

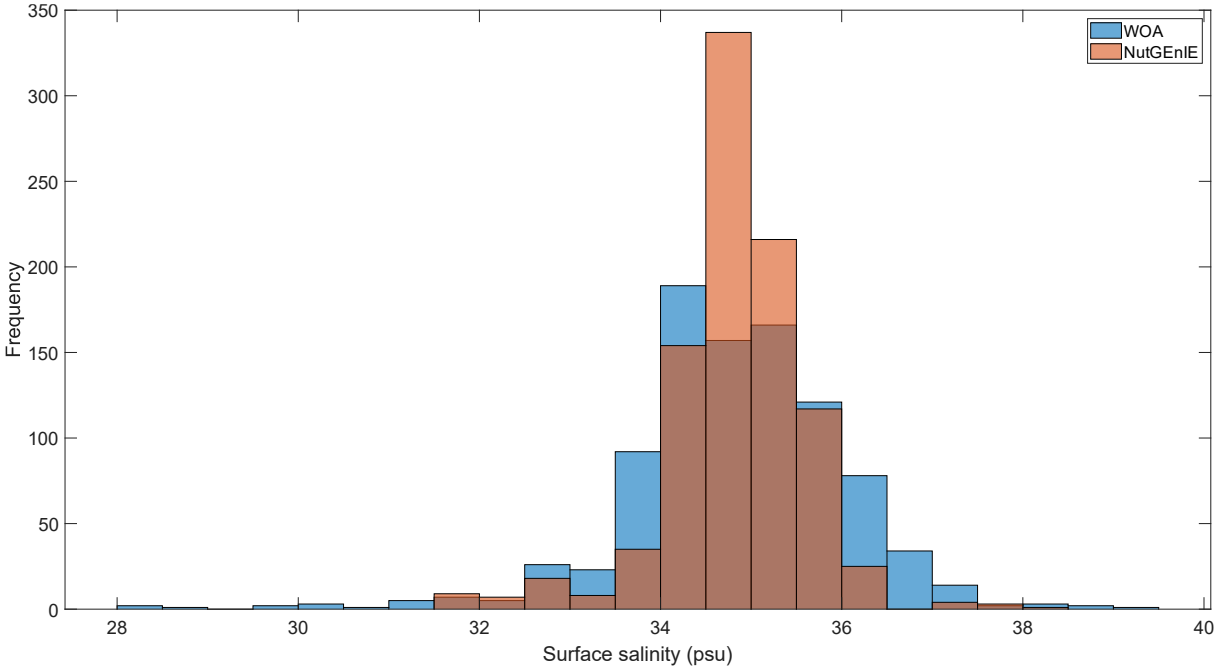

Figure S32 Histogram of NutGEnIE and WOA surface salinity. NutGEnIE shown in orange, WOA shown in blue. Salinity values in psu.

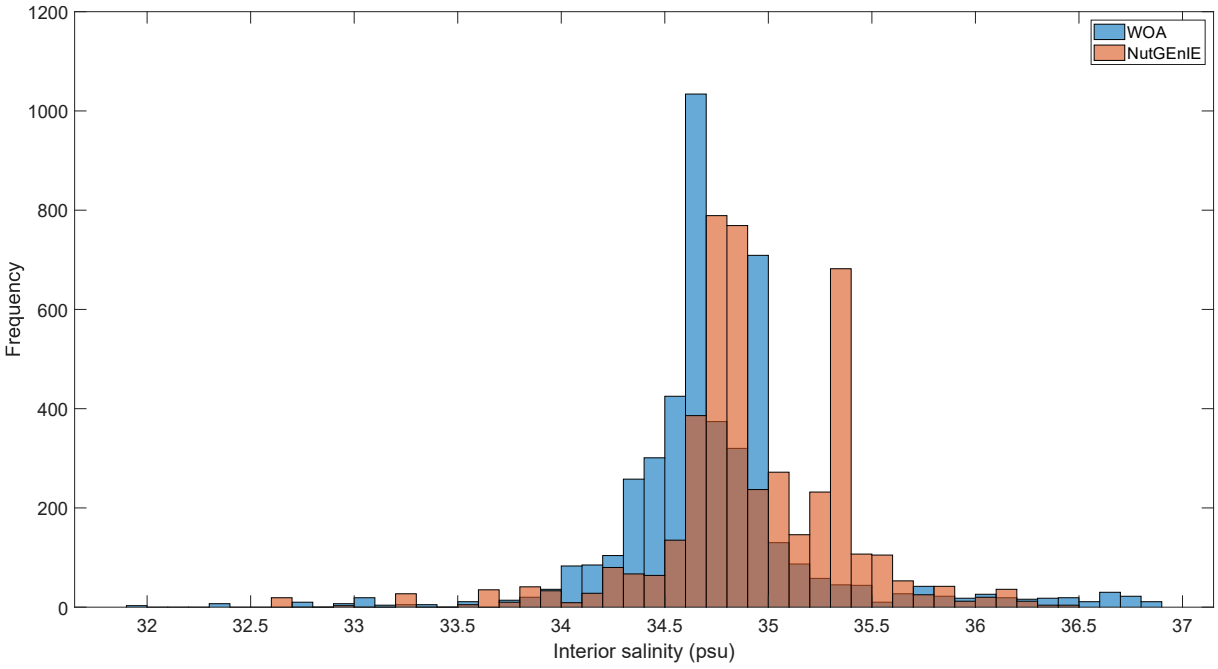

Figure S33 Histogram of NutGEnIE and WOA interior salinity. NutGEnIE shown in orange, WOA shown in blue. Salinity values in psu.

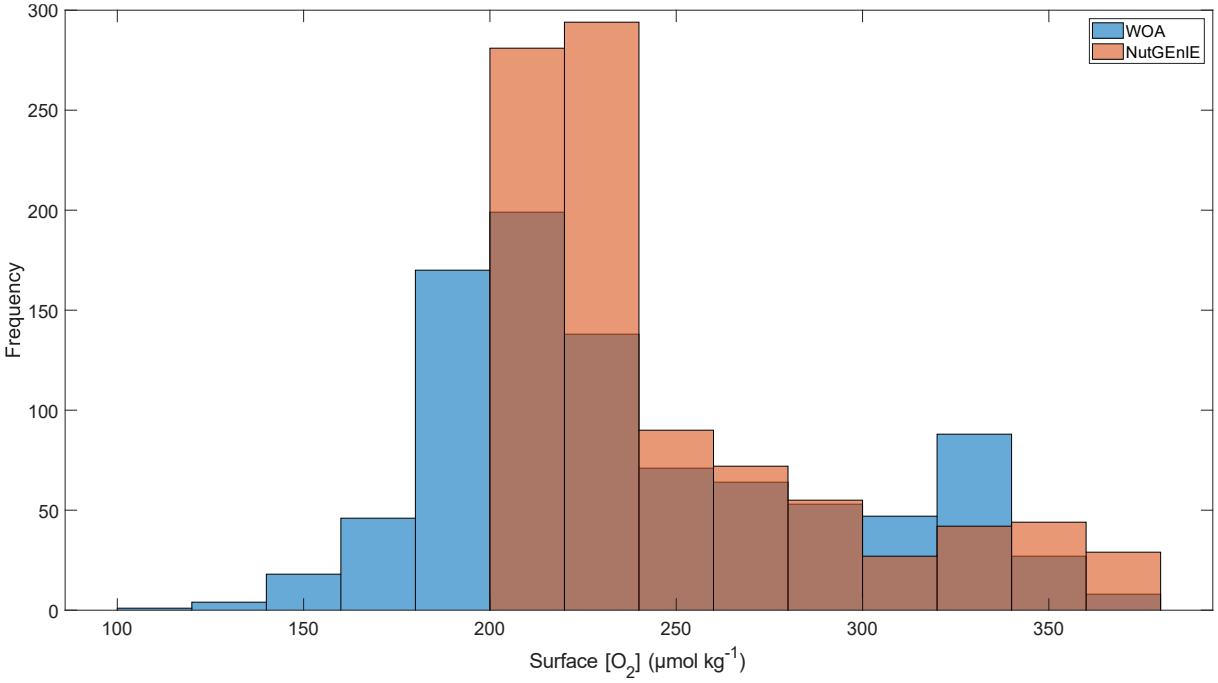

Figure S34 Histogram of NutGEnIE and WOA surface [O_2]. NutGEnIE shown in orange, WOA shown in blue. Concentration values in µmol kg^{-1}.

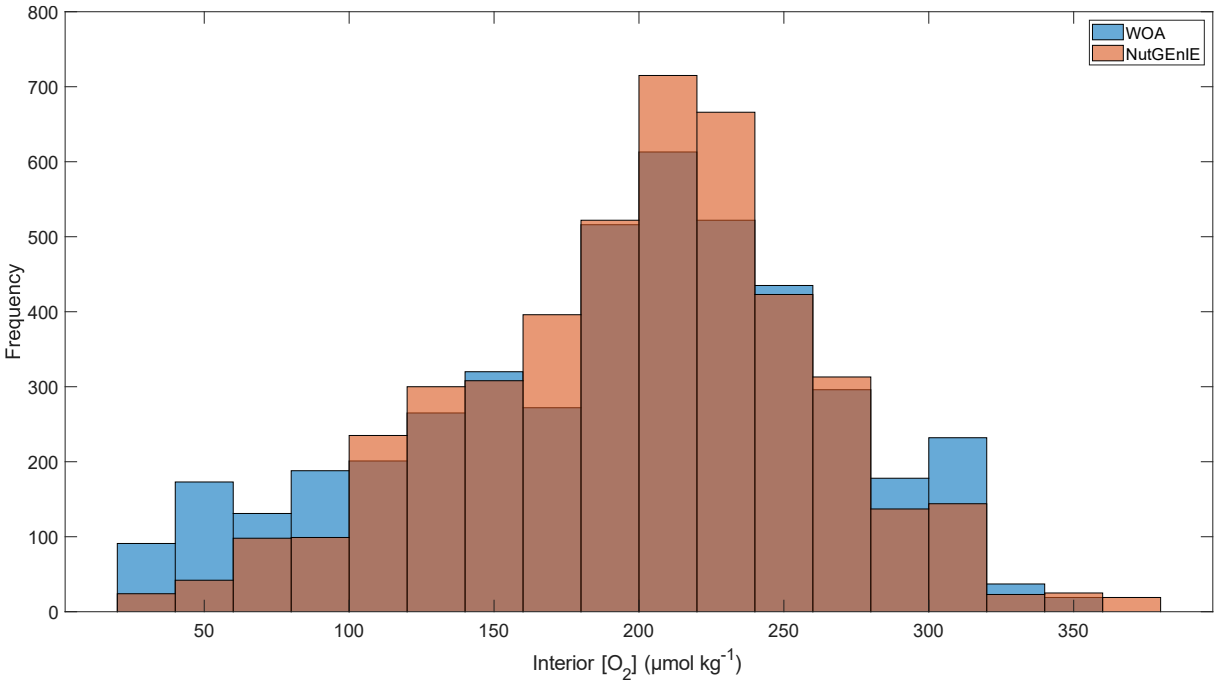

Figure S35 Histogram of NutGEnIE and WOA interior [O_2]. NutGEnIE shown in orange, WOA shown in blue. Concentration values in µmol kg^{-1}.

S2.7. Ocean productivity.

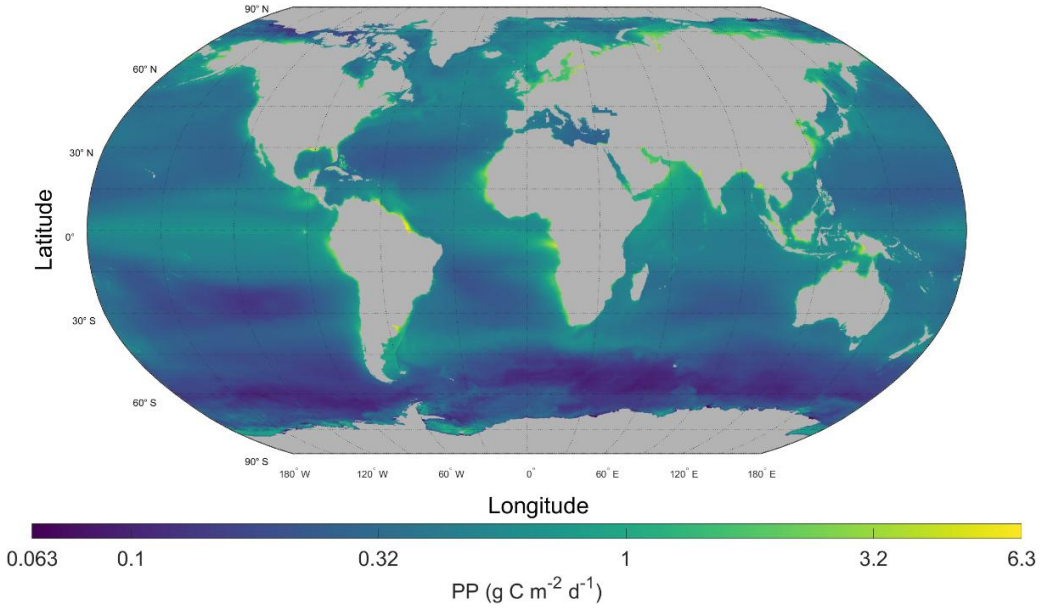

Figure S36 Annual mean global primary production. Based on the dataset from Oregon State University Ocean Productivity (Ocean Productivity, 2024). In this figure the dataset has not been re-gridded to match the NutGEnIE grid.

S2.8. Nutrient uptake limiting factors.

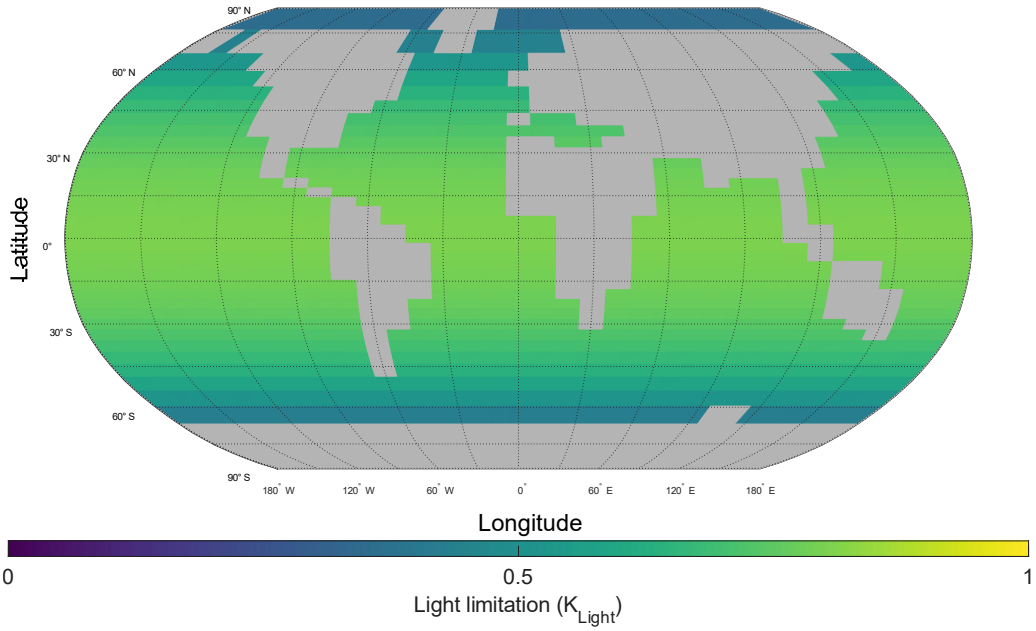

Figure S37 Spatial variation of light limiting factor for nutrient uptake. For other phytoplankton and diazotrophs. Lower values indicate that light is more limiting to nutrient uptake. K_{Light} is equivalent to the $\boldsymbol{\gamma^{l}}$ term in Eq. (3) and (4).

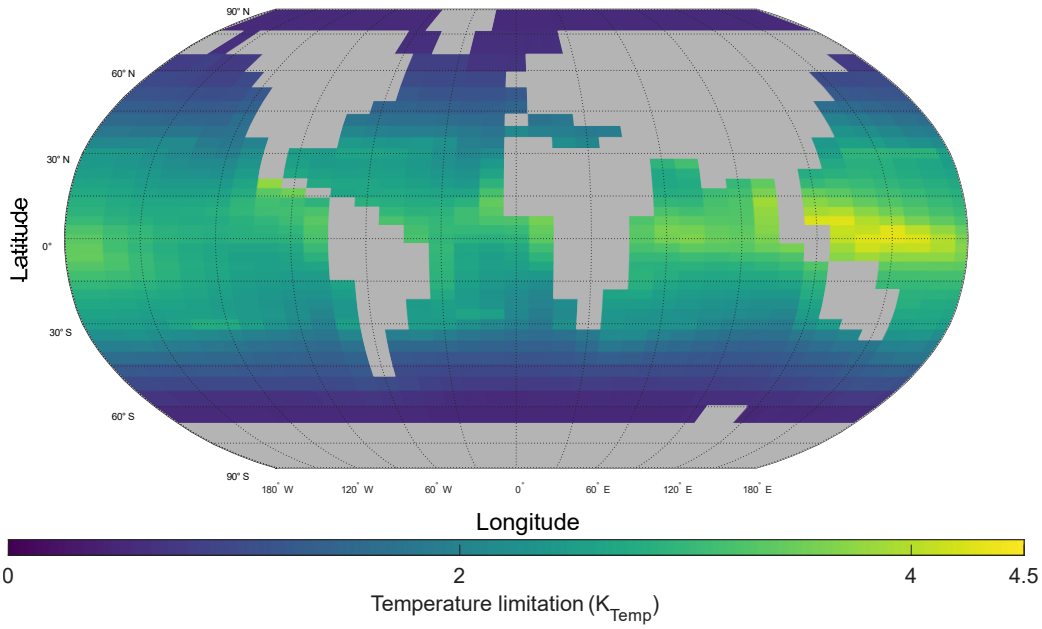

Figure S38 Spatial variation of temperature limiting factor for nutrient uptake. For other phytoplankton and diazotrophs. Lower values indicate that temperature is more limiting to nutrient uptake. K_{Temp} is equivalent to the $\boldsymbol{\gamma^T}$ term in Eq. (3) and (4).

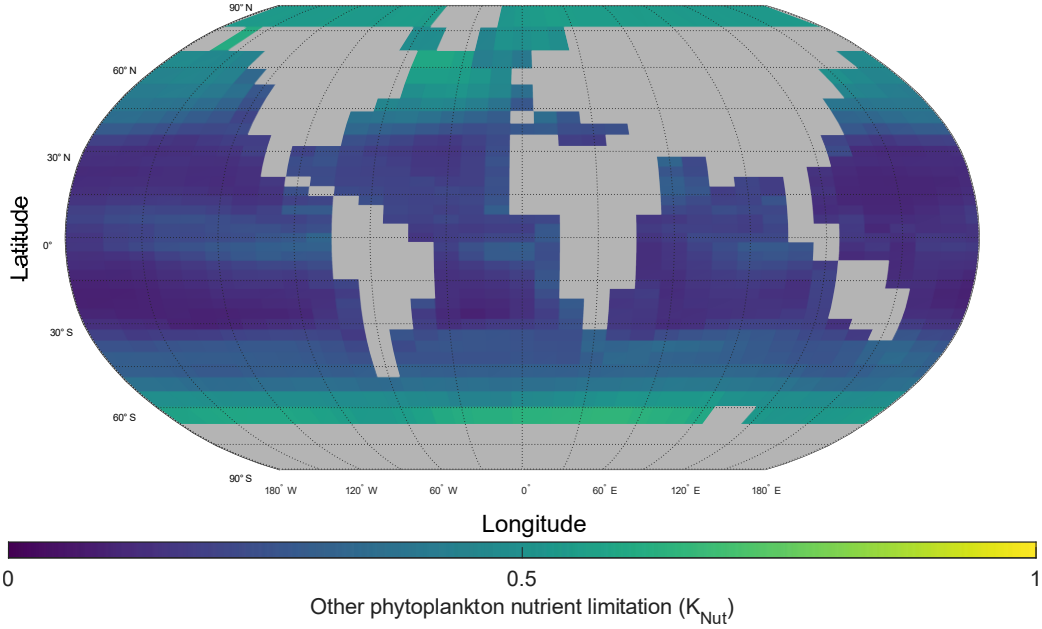

Figure S39 Spatial variation of nutrient limiting factor for nutrient uptake by other phytoplankton. For other phytoplankton. Lower values indicate that nutrient supply is more limiting to nutrient uptake by other phytoplankton. K_{Nut} is equivalent to the $\boldsymbol{min}\left[\frac{PO_4^{3-}}{PO_4^{3-}+K_P}; \frac{DIN}{DIN+K_N}; \frac{Fe_T}{Fe_T+K_{Fe}}\right]$ term in Eq. (3).

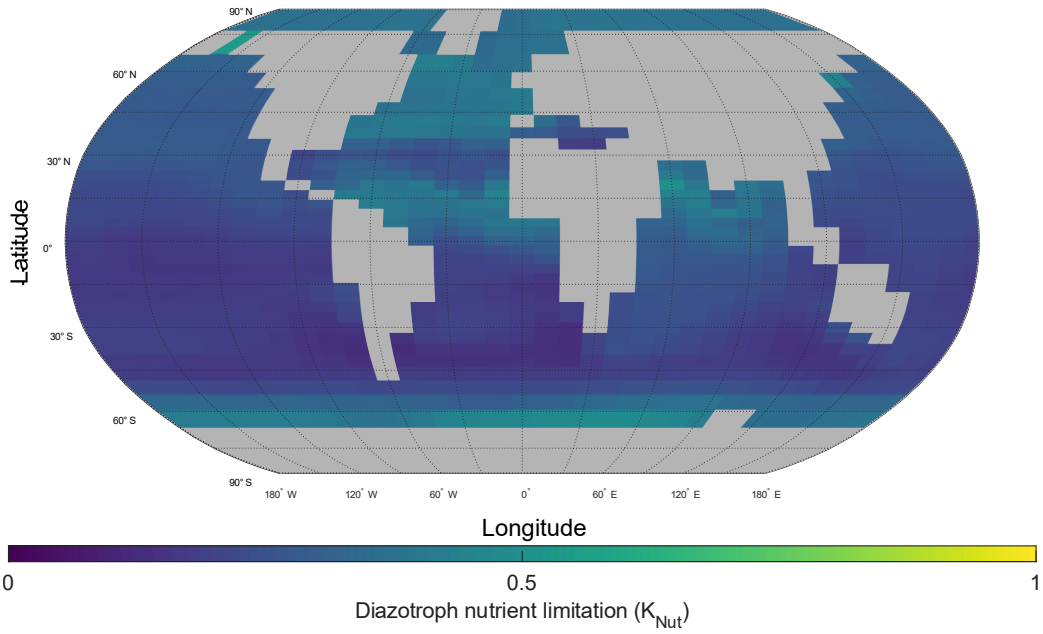

Figure S40 Spatial variation of nutrient limiting factor for nutrient uptake by diazotrophs. For diazotrophs. Lower values indicate that nutrient supply is more limiting to nutrient uptake by other diazotrophs. K_{Nut} is equivalent to the $\boldsymbol{min}\left[\frac{PO_4^{3-}}{PO_4^{3-}+K_P}; \frac{Fe_T}{Fe_T+K_{Fe}^{Diaz}}\right]$ term in Eq. (4).

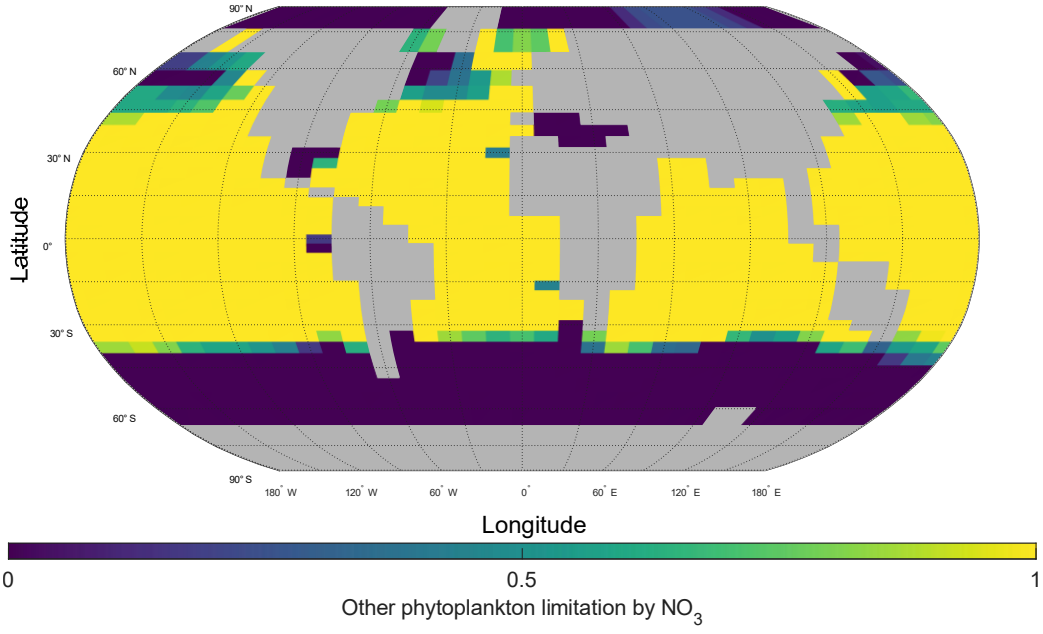

Figure S41 Spatial variation of NO_3 limitation for nutrient uptake by other phytoplankton. For other phytoplankton. 0 = no NO_3^- limitation, 0.5 = NO_3^- limitation 50 % of time, 1 = NO_3^- limitation 100 % of time.

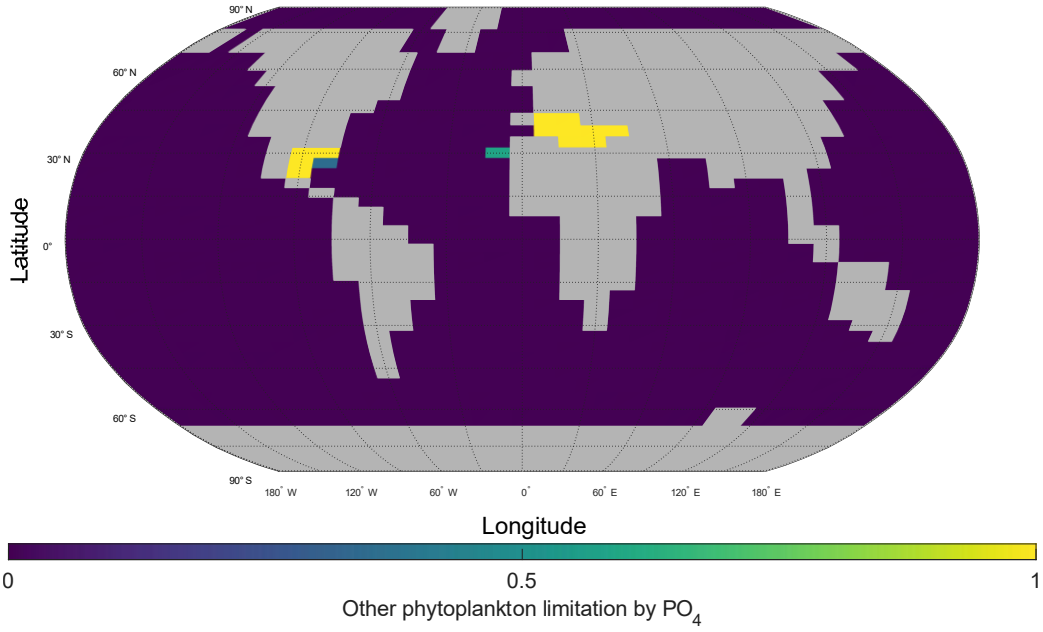

Figure S42 Spatial variation of PO_4 limitation for nutrient uptake by other phytoplankton. For other phytoplankton. 0 = no PO_4^{3-} limitation, 0.5 = PO_4^{3-} limitation 50 % of time, 1 = PO_4^{3-} limitation 100 % of time.

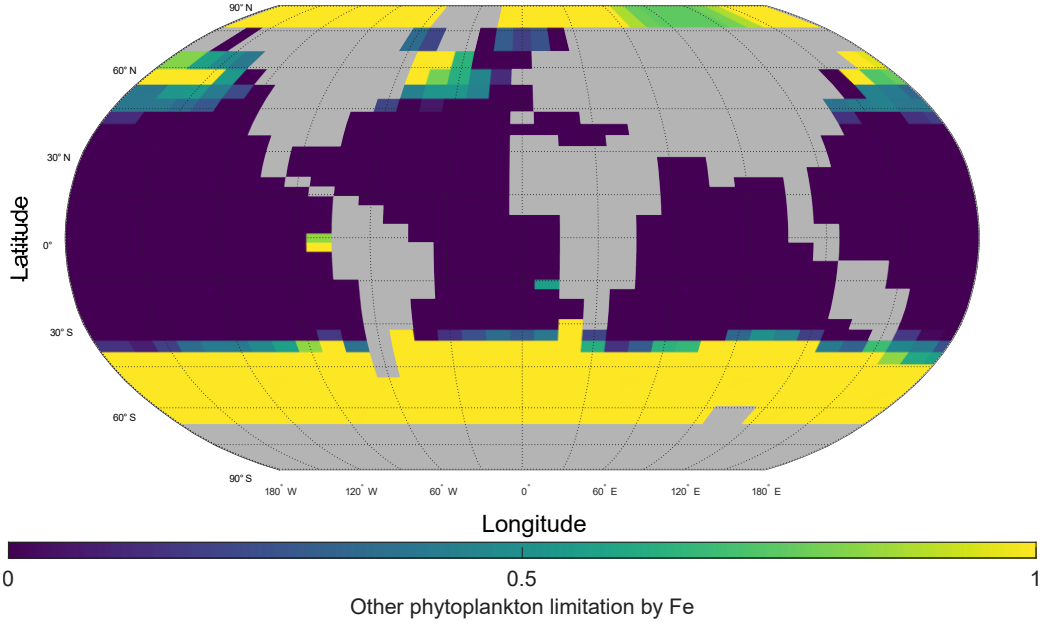

Figure S43 Spatial variation of Fe limitation for nutrient uptake by other phytoplankton. For other phytoplankton. 0 = no Fe limitation, 0.5 = Fe limitation 50 % of time, 1 = Fe limitation 100 % of time.

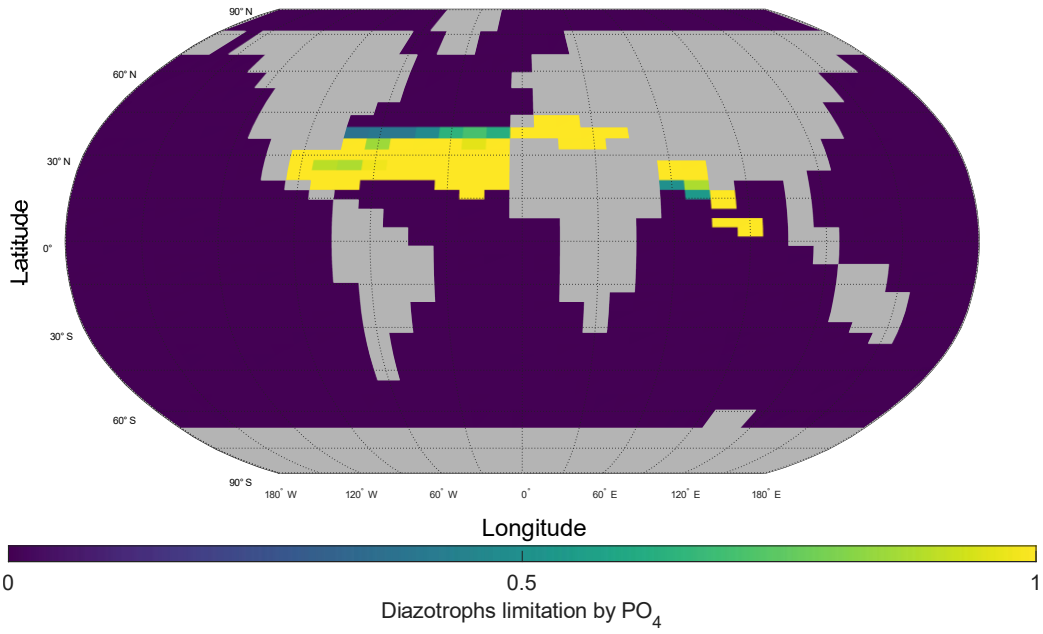

Figure S44 Spatial variation of PO_4 limitation for nutrient uptake by other diazotrophs. For diazotrophs. 0 = no PO_4^{3-} limitation, 0.5 = PO_4^{3-} limitation 50 % of time, 1 = PO_4^{3-} limitation 100 % of time.

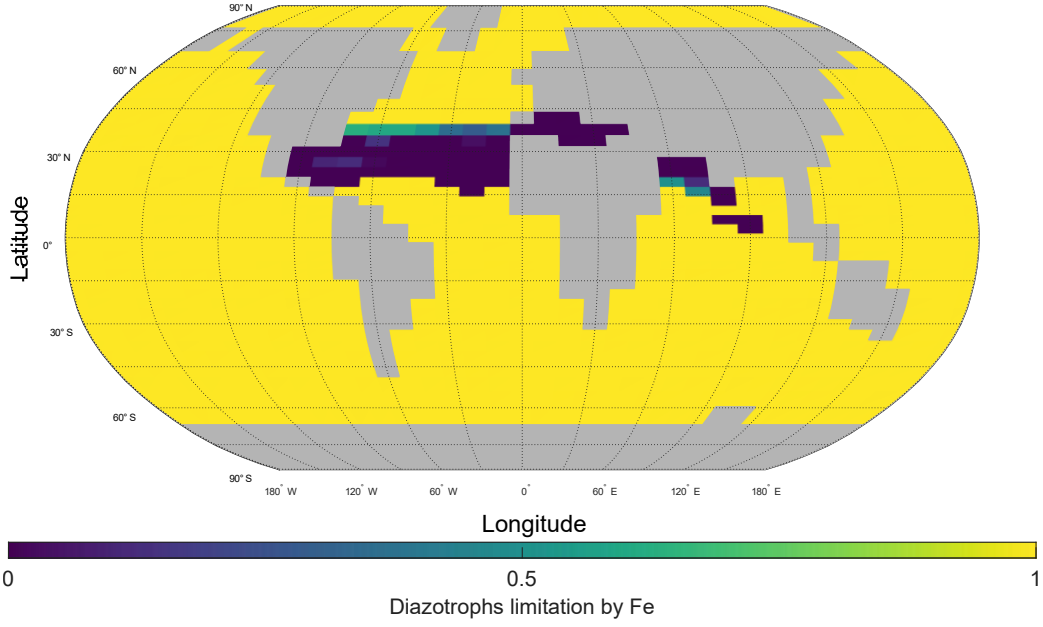

185 **Figure S45 Spatial variation of Fe limitation for nutrient uptake by diazotrophs**. For diazotrophs. 0 = no Fe limitation, 0.5 = Fe limitation 50 % of time, 1 = Fe limitation 100 % of time.

S2.9. Spatial variation of nutrient limiting values.

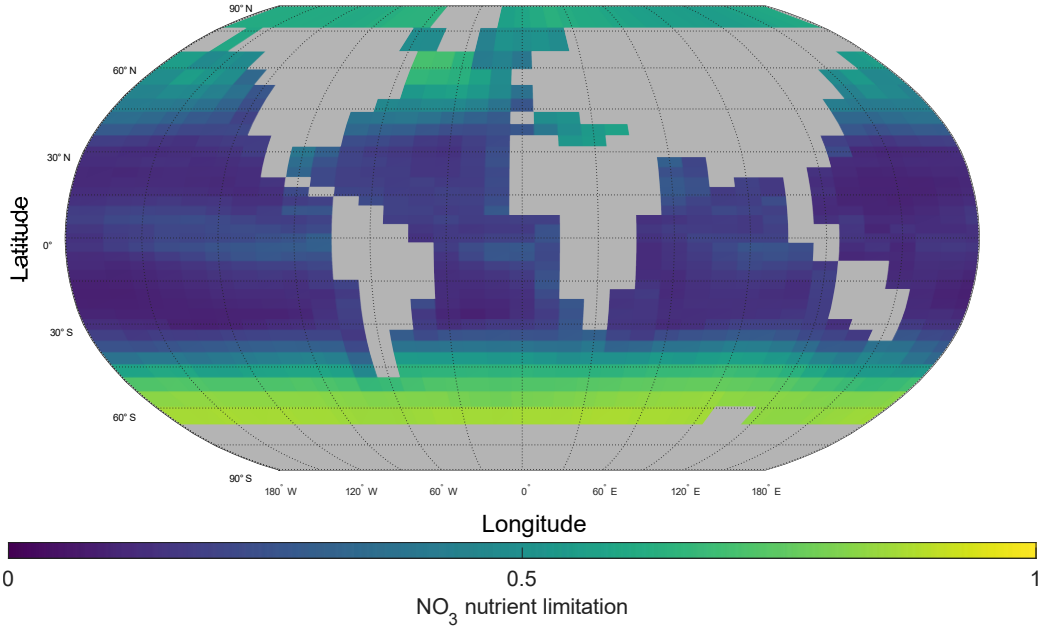

Figure S46 Spatial variation of NO_3^- limitation value. Limitation value for NO_3^- is calculated by $\frac{\mathbf{DIN}}{\mathbf{DIN+K_N}}$.

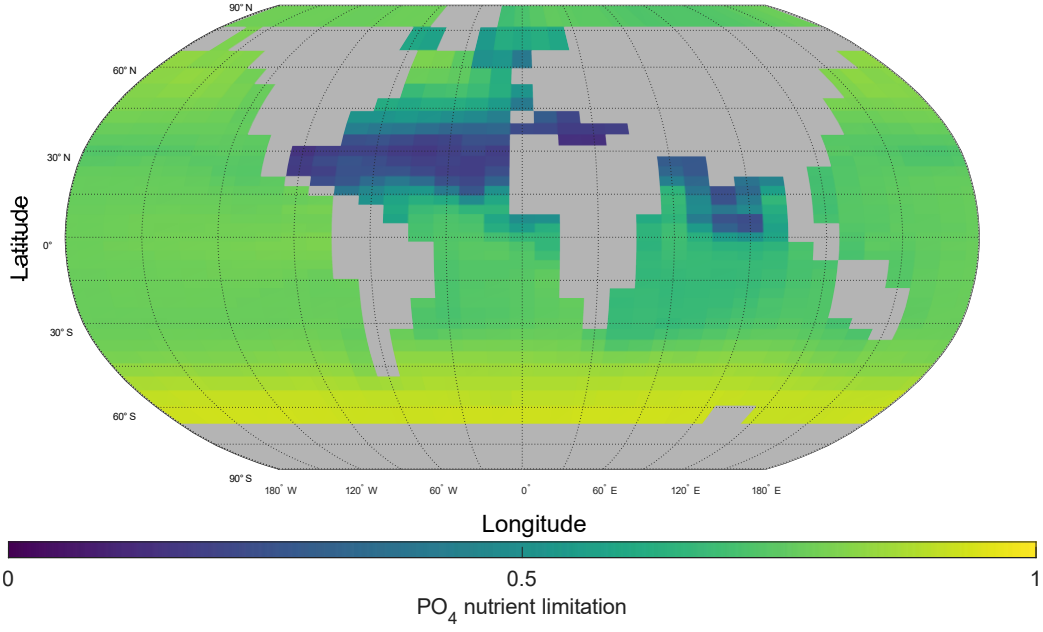

190

Figure S47 Spatial variation of PO_4^{3-} limitation value. Limitation value for PO_4^{3-} is calculated by $\frac{PO_4^{3-}}{PO_4^{3-}+\boldsymbol{K_P}}$.

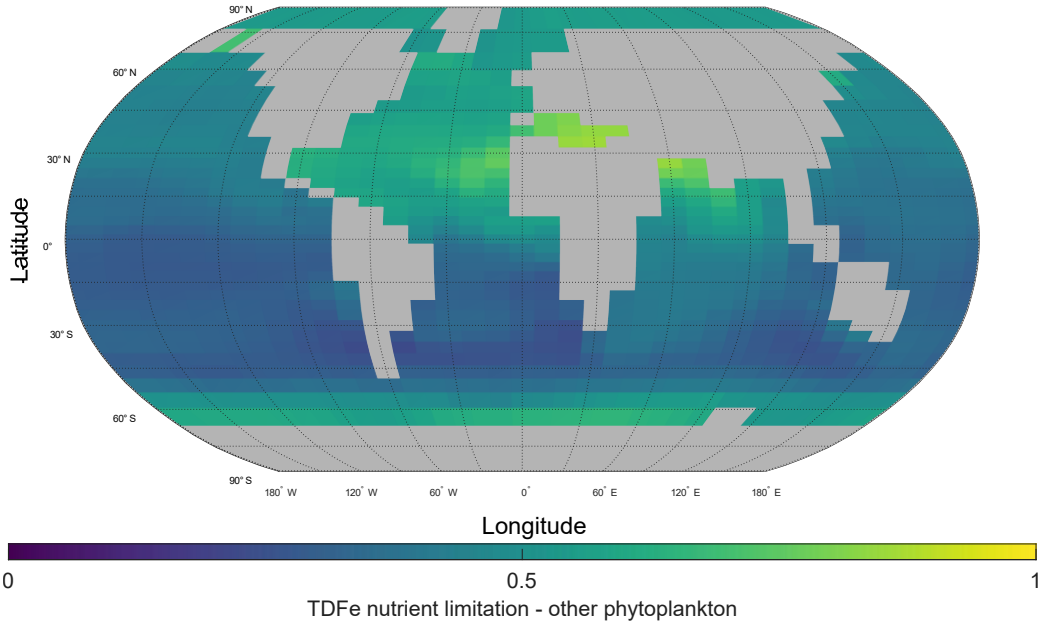

Figure S48 Spatial variation of Fe limitation value for other phytoplankton. Limitation value for Fe is calculated by $\frac{Fe}{Fe+K_{Fe}}$.

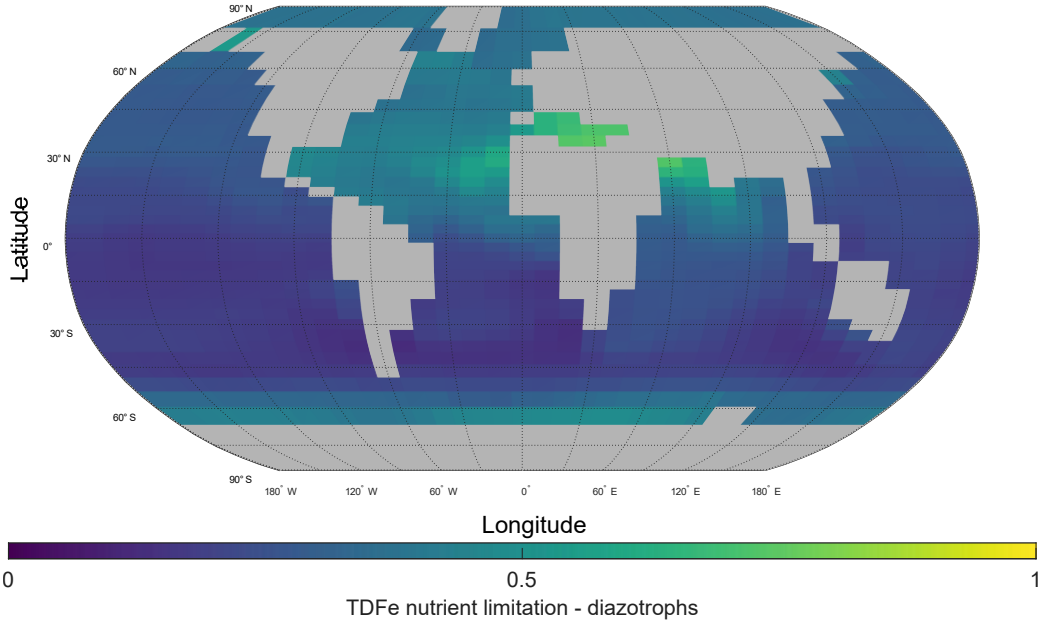

Figure S49 Spatial variation of Fe limitation value for diazotrophs. Limitation value for Fe is calculated by $\frac{Fe}{Fe+K_{Fe}^{Diaz}}$.

S2.10. Apparent Oxygen Utilisation (AOU) transects

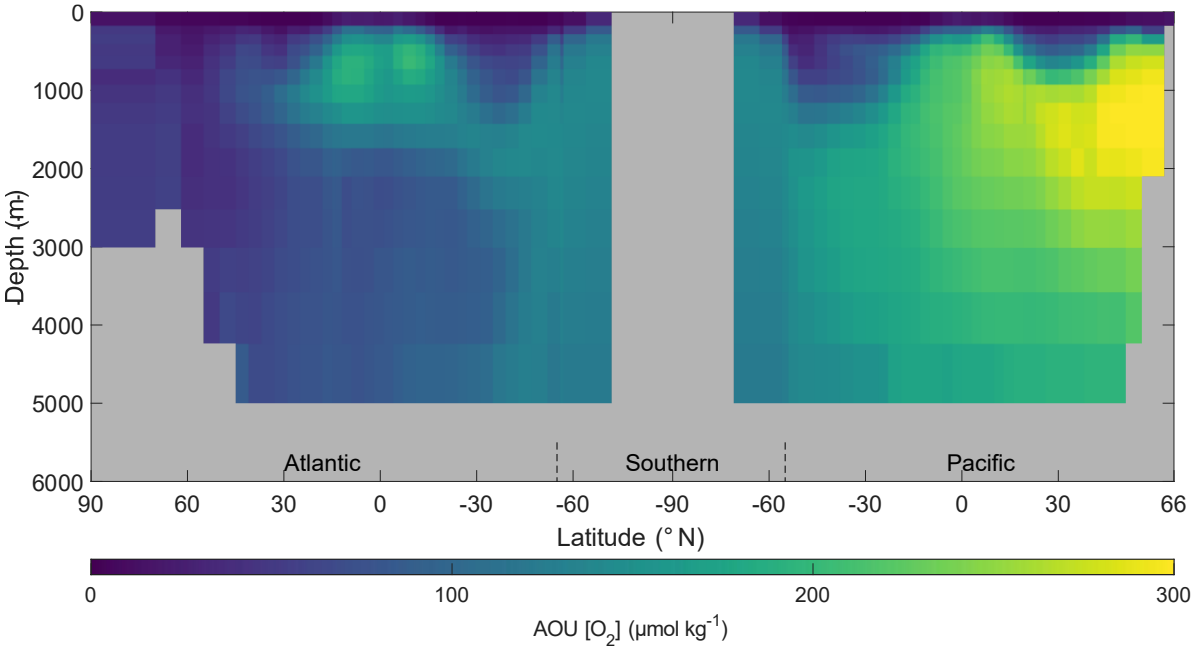

Figure S50 World Ocean Atlas annual mean global Apparent Oxygen Utilisation (AOU). Observed World Ocean Atlas Re-gridded (WOAR) thermohaline transect zonal mean AOU in µmol kg^{-1}.

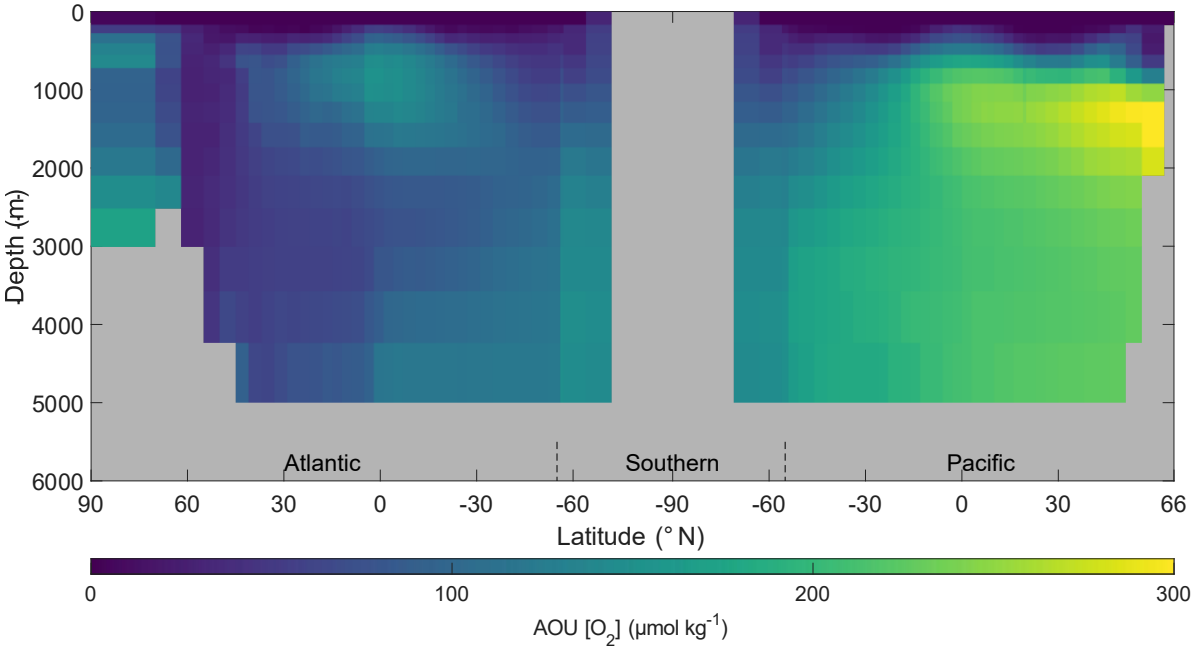

200

Figure S51 NutGEnIE annual mean global Apparent Oxygen Utilisation (AOU). NutGEnIE thermohaline transect zonal mean AOU in µmol kg^{-1}.

S2.11. Nitrogen* transects

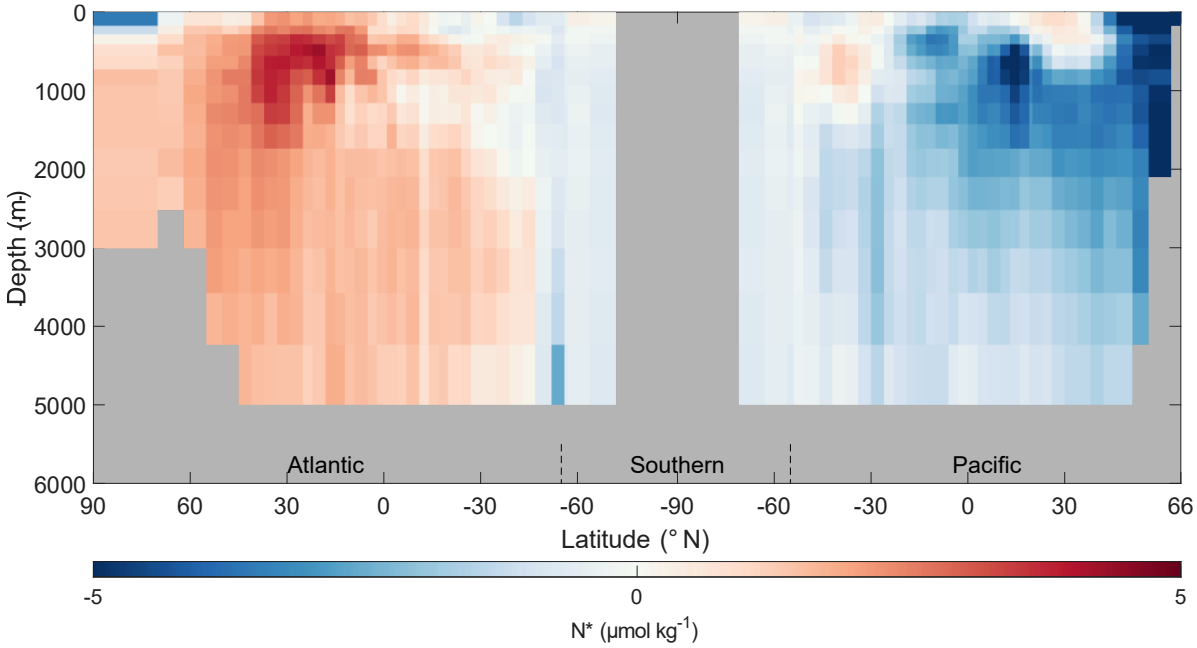

Figure S52 World Ocean Atlas annual mean global Nitrogen*. Observed World Ocean Atlas Re-gridded (WOAR) thermohaline transect zonal mean Nitrogen* in µmol kg^{-1}.

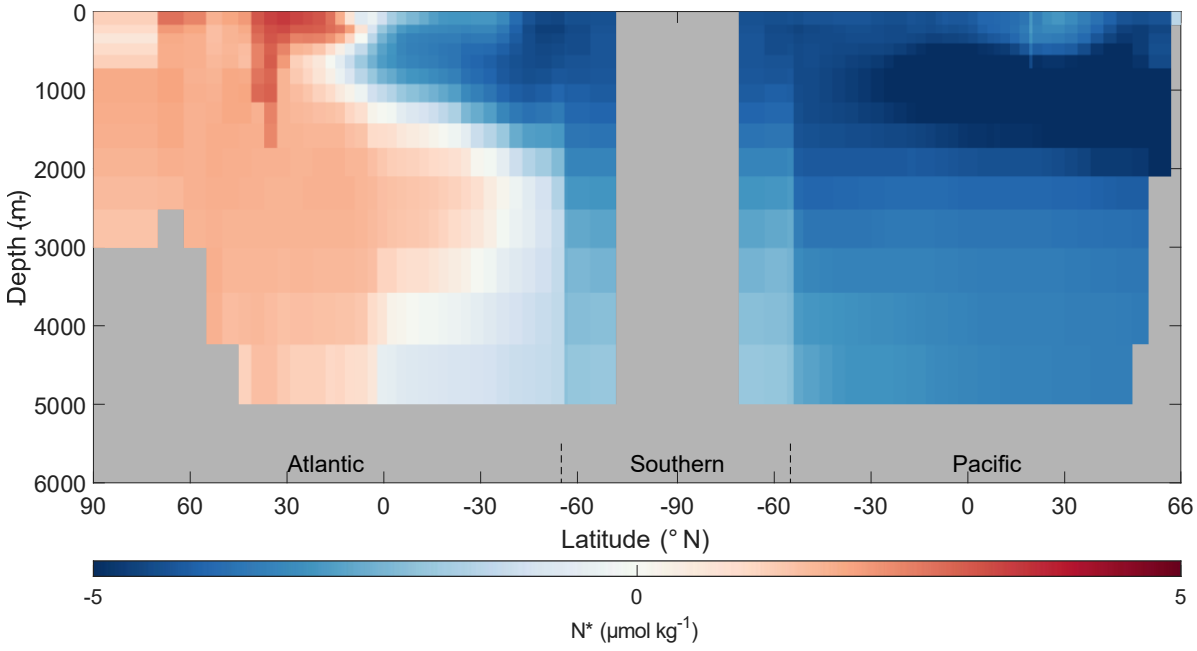

Figure S53 NutGEnIE annual mean global Nitrogen*. NutGEnIE thermohaline transect zonal mean Nitrogen* in µmol kg^{-1}.

S3. Supplementary tables

Table S1 Depth of NutGEnIE ocean layers. The depth (m) at the base of each layer, with 1 being the surface layer and 16 the deepest possible layer.

layer	Base of layer (m)
1	80.84
2	174.75
3	283.85
4	410.58
5	557.80
6	728.83
7	927.51
8	1158.31
9	1426.43
10	1737.90
11	2099.73
12	2520.05
13	3008.34
14	3575.57
15	4234.52
16	5000.00

Table S2 Configured atmospheric and ocean tracers of NutGEnIE. The prefixes of the TracerIDs refer to atmospheric (atm) and ocean (ocn). For each tracer the initial value and units are provided. Additional tracers are enabled without the need for configuration such as temperature and salinity. Initial values are provided to a maximum of 2 decimal places, exact values may be specified to greater precision.

TracerID	Tracer	Description	Initial value	Units
atm 3	*p*CO2	carbon dioxide	278×10^{-6}	atm
atm 4	*p*CO2_13C	d13C portion of *p*CO2	-6.5	o/oo
atm 6	*p*O2	oxygen	0.21	Atm
atm 16	*p*H2S	hydrogen sulphide	0.0	atm
ocn 3	DIC	dissolved inorganic carbon	2.24×10^{-3}	mol kg^{-1}
ocn 4	DIC_13C	d13C portion of DIC	0.4	o/oo
ocn 6	NO3	dissolved nitrate	3.16×10^{-5}	mol kg^{-1}
ocn 8	PO4	dissolved phosphate	2.16×10^{-6}	mol kg^{-1}
ocn 10	O2	dissolved oxygen	1.70×10^{-4}	mol kg^{-1}
ocn 12	ALK	total alkalinity	2.36×10^{-3}	mol kg^{-1}
ocn 15	DOM_C	dissolved organic matter; carbon	1.44×10^{-6}	mol kg^{-1}
ocn 16	DOM_C_13C	d13C portion of DOM_C	-29.66	o/oo
ocn 18	DOM_N	DOM; nitrogen	2.17×10^{-7}	mol kg^{-1}
ocn 20	DOM_P	DOM; phosphorous	1.36×10^{-8}	mol kg^{-1}
ocn 22	DOM_Fe	DOM; iron	8.94×10^{-12}	mol kg^{-1}
ocn 28	NH4	dissolved ammonium	7.30×10^{-8}	mol kg^{-1}
ocn 30	N2	dissolved nitrogen	6.96×10^{-9}	mol kg^{-1}
ocn 90	TDFe	total dissolved iron	6.50×10^{-10}	mol kg^{-1}
ocn 42	TL	total dissolved ligand	1.00×10^{-9}	mol kg^{-1}
ocn 35	Ca	dissolved calcium	1.03×10^{-2}	mol kg^{-1}
ocn 38	SO4	dissolved sulphate	2.92×10^{-2}	mol kg^{-1}
ocn 40	H2S	dissolved hydrogen sulphide	7.89×10^{-9}	mol kg^{-1}
ocn 50	Mg	dissolved magnesium	5.28×10^{-2}	mol kg^{-1}

References

Garcia, H., Weathers, K., Paver, C., Smolyar, I., Boyer, T., Locarnini, M., Zweng, M., Mishonov, A., Baranova, O., and Seidov, D.: World ocean atlas 2018, Volume 3: Dissolved Oxygen, Apparent Oxygen Utilization, and Dissolved Oxygen Saturation, 2018.

Garcia, H. E. and Gordon, L. I.: Oxygen solubility in seawater: Better fitting equations, Limnology and Oceanography, 37, 1307-1312, https://doi.org/10.4319/lo.1992.37.6.1307, 1992.

Gruber, N. and Sarmiento, J. L.: Global patterns of marine nitrogen fixation and denitrification, Global Biogeochemical Cycles, 11, 235-266, https://doi.org/10.1029/97GB00077, 1997.

Mahowald, N. M., Muhs, D. R., Levis, S., Rasch, P. J., Yoshioka, M., Zender, C. S., and Luo, C.: Change in atmospheric mineral aerosols in response to climate: Last glacial period, preindustrial, modern, and doubled carbon dioxide climates, Journal of Geophysical Research: Atmospheres, 111, https://doi.org/10.1029/2005JD006653, 2006.

Matsumoto, K., Tokos, K., Huston, A., and Joy-Warren, H.: MESMO 2: a mechanistic marine silica cycle and coupling to a simple terrestrial scheme, Geosci. Model Dev., 6, 477-494, https://doi.org/10.5194/gmd-6-477-2013, 2013.

Ocean Productivity: http://orca.science.oregonstate.edu/index.php, last access: 1 June 2024.